UC Berkeley
UC Berkeley Previously Published Works

Title
Coupled-Cluster Valence-Bond Singles and Doubles for Strongly Correlated Systems: Block-Tensor Based Implementation and Application to Oligoacenes.

Permalink
https://escholarship.org/uc/item/17t2n836

Journal
Journal of chemical theory and computation, 13(2)

ISSN
1549-9618

Authors
Lee, Joonho
Small, David W
Epifanovsky, Evgeny
et al.

Publication Date
2017-02-01

DOI
10.1021/acs.jctc.6b01092

Peer reviewed

Coupled-Cluster Valence-Bond Singles and Doubles for Strongly Correlated Systems: Block-Tensor Based Implementation and Application to Oligoacenes

SCHOLARONE™
Manuscripts

Coupled-Cluster Valence-Bond Singles and Doubles for Strongly Correlated Systems: Block-Tensor Based Implementation and Application to Oligoacenes

Joonho Lee, David W. Small,* Evgeny Epifanovsky, and Martin Head-Gordon*

Department of Chemistry, University of California, Berkeley, California 94720, USA

Chemical Sciences Division, Lawrence Berkeley National Laboratory, Berkeley, California 94720, USA

E-mail: dsmallchem@gmail.com; mhg@cchem.berkeley.edu

Abstract

We demonstrate a block-tensor based implementation of coupled-cluster valence-bond singles and doubles (CCVB-SD) [*J. Chem. Phys.* **2012**, *137*, 114103] which is a simple modification to restricted CCSD (RCCSD) that provides a qualitatively correct description of valence correlations even in strongly correlated systems. We derive the Λ-equation of CCVB-SD and the corresponding unrelaxed density matrices. The resulting production-level implementation is applied to oligoacenes, correlating up to 318 electrons in 318 orbitals. CCVB-SD shows a qualitative agreement with exact methods for short acenes and reaches the bulk limit of oligoacenes in terms of natural orbital occupation numbers whereas RCCSD shows non-variational behaviour even for relatively short acenes. A significant reduction in polyradicaloid character is found when correlating all valence electrons instead of only the π-electrons.

Introduction

Strong correlations are an important subject of active research in the field of electronic structure theory. Systems with d or f orbitals such as metalloenzymes[1] like photosystem II[2,3] are well known strongly correlated systems. Polyradicaloid systems such as molecules near bond-breaking[4] and polyaromatic hydrocarbons,[5–9] also belong to this category. Phenomena driven by correlations between electrons that lie outside perturbative regimes such as high-T_C superconductivity[10] and Kondo problems[11] are also inherently strong correlation problems. Describing these systems and phenomena requires proper treatment of strong correlations to obtain at least a qualitatively correct description.

One of the most popular approaches in quantum chemistry to address these problems is the use of brute-force algorithms such as complete active space self-consistent field (CASSCF).[12] The applicability of CASSCF is limited by the need to solve the full configuration interaction (FCI) problem within an active space, which has a computational cost that scales exponentially with the number of electrons in the active space. To extend the applicability of CASSCF, enormous efforts have been made on developing more efficient approximate FCI solvers such as Alavi and co-worker's FCI quantum monte carlo (FCIQMC)[13,14] and White's density matrix renormalisation group (DMRG).[15–19] FCIQMC uses importance sampling techniques of QMC to solve the FCI problem and shows a weaker exponential scaling compared to the traditional determinant based exact FCI solver.[20,21] DMRG was originally designed for solving one-dimensional (1D) lattice systems and encodes the most important degrees of freedom between neighbouring sites using singular value decompositions of density matrices. DMRG is a polynomial-scaling method for 1D systems with short-range interactions, but is still an exponential-scaling method for general systems of higher dimensions or with long-range interactions. These two independent approaches have been applied to non-trivial chemical systems small enough to afford these brute force approaches.[22–29] It is, however, highly desirable to develop polynomial-scaling methods that can qualitatively capture strong correlations in systems where FCIQMC and DMRG become intractable.

Another common approach to strong correlations is multi-reference coupled-cluster (MRCC) theory.[30–32] The basic idea is to include physically relevant higher cluster excitations by employing multiple determinants in the reference state that are difficult to access in the usual single reference approaches. MRCC approaches can be categorised into (1) state-universal[33–38] and (2) valence-universal[39–47] that are often referred to as genuine MRCC approaches and (3) state-specific approaches.[48–71] The first two suffer from the appearance of intruder states[72–75] and require solving for several eigenstates simultaneously, many of which can be irrelevant to the problem. The third approach can avoid these problems but usually at the expense of the explicit inclusion of higher excitations. These are still active areas of research in the pursuit of strong correlations, and interested readers are referred to ref. 31 and references therein.

Another interesting, formally simpler, and often computationally more tractable approach than those mentioned above, is single-reference coupled-cluster (SRCC) theory. SRCC singles and doubles with non-iterative triples (CCSD(T)) is a *de facto* standard approach for non-strongly correlated systems.[76] Its non-variational failure for strongly correlated systems when used with restricted Hartree-Fock (RHF) references has inspired development of new methods.

The simplest possible (and thus the most widely used) fix to this problem is to use an unrestricted HF (UHF) reference at the expense of spin symmetry. However, many studies have indicated that UCCSD or UCCSD(T) misses a fair amount of correlations in the so-called spin-recoupling regime, an intermediate regime between equilibrium and bond-dissociation.[77] More crucially, these methods fail to provide quantitatively accurate singlet-triplet gaps due to severe spin contaminations. Using UHF references is thus not satisfying for general applications.

An alternative approach without increasing the substitution level (i.e. with only singles and doubles substitutions), is to correct for higher excitations in a non-iterative fashion. This is done in the methods of moments coupled cluster approximations including renor-

malised and completely renormalised variants.[78–86] Instead of evaluating the energy using projection equations, more stable approaches include evaluating it variationally with either an expectation value ansatz[87–89] or a unitary ansatz[90–93] and approximations to the variational evaluation such as extended CC (ECC)[94–99] and quadratic CC (QCC).[100–102] These have shown improved energetics in strongly correlated systems, but none of them are an ultimate solution to the problem. Increasing the substitution levels systematically, such as up to triples (RCCSDT)[103] and up to quadruples (RCCSDTQ),[104] is another approach at the expense of steep scaling costs ($n_{occ}^3 n_{vir}^5$ and $n_{occ}^4 n_{vir}^6$, respectively).

Recently, our group has developed a local correlation model for strong correlations, the hierarchical perfect n-tuples model (e.g. perfect quadruples (PQ), perfect hextuples (PH), etc.).[105–108] It explicitly incorporates higher cluster operators up to n-tuples in a very restricted form to better preserve computational feasibility. The use of localised orbitals is essential in this approach as the limited number of higher excitations will be most effective among orbitals that are spatially close. The price we pay for this is that the energy is no longer invariant with respect to occupied-occupied and virtual-virtual rotations. Moreover, simultaneous multiple bond-breaking will require a higher n-tuples model, which becomes intractable quickly.

Another simple and yet very effective approach are the spin-flip methods pioneered by Krylov and co-workers.[109–112] Equation-of-motion spin-flip coupled cluster (EOM-SF-CC) theory is based on the observation that restricted open-shell HF (ROHF) can qualitatively describe strongly correlated systems in a high-spin state such as triplet stretched H_2. At the level of singles and doubles, EOM-SF-CCSD describes the singlet ground state as an excitation or a deexcitation from a high-spin CCSD wavefunction. It has been widely used for diradical systems.[110] The major drawback of this approach is that systems with many strongly correlated electrons would require the use of extremely high-spin reference whose orbitals are far from being suitable to describe singlet ground states.

There have been proposals that remove certain quadratic terms in doubles (D) amplitudes

equations in RCCSD to mimic the effects of triples and quadruples (TQ) and greatly improve the accuracy for strongly correlated systems. Many of them were originally motivated by the cost reduction when ignoring some non-linear terms, but later it was realised that discarding such terms can vastly improve the accuracy in molecules near quasi-degeneracy. The main goal in this research direction is to account approximately for higher excitations (T, Q, ...) whilst retaining formal properties of RCCSD such as size-extensivity, energy-invariance with respect to occupied-occupied and virtual-virtual rotations, and exactness for non-interacting two electron systems.

This approach was pioneered by Paldus and co-workers who developed approximate coupled-pairs with quadruples (ACPQ)[113,114] which has inspired many subsequent developments. ACPQ was motivated by the structure of Q extracted from a cluster analysis of a broken-symmetry wavefunction such as UHF and projected HF (PHF), which cancels certain quadratic terms when studying strongly correlated limits of the Pariser-Parr-Pople model.[114] This provided justification for related approaches such as ACP-D45[115,116] and approximate CCD (ACCD)[117,118]. Linearised CC,[119] 2CC,[120] and coupled electron pair approximation (CEPA) and its variants[121,122] also belong to this category.

A more recent approach in this category is the distinguishable cluster approximation (DCA)[123] where a diagram corresponding to direct exchange of two doubles amplitudes is discarded. It was suggested as an *ad hoc* modification to RCCD (called DCD) and later derived from a screened Coulomb formalism.[124] DCD and its variants (Brueckner DCD, orbital-optimised DCD and DCSD)[123–126] all do not "turn over" when breaking N_2. Despite its promising earlier results its non-interative triples version (DCSD(T)) shows a similar non-variational failure to that of CCSD(T) for bond-breaking[124] when applied to N_2. This suggests that an alternative way to include T perhaps in an iterative fashion should be explored.

Another recent approach in this category is singlet-paired CCSD (CCSD0) proposed by Bulik *et al.*[127] The singlet doubles operator in RCCSD can be divided into symmetric singlet

doubles (or singlet-pairing doubles) and antisymmetric singlet doubles (or triplet-pairing doubles). This splitting of the doubles operator was extensively exploited in orthogonally spin adapted formula,[128–131] and it will be reviewed later in this paper as well. In CCSD0, the antisymmetric singlet doubles operator is completely removed by ansatz. Removing those terms improves the performance of the theory for bond dissociations, although when applied to N_2 in a minimal basis it does not reach the correct asymptote.[132] Moreover, the contribution from the removed antisymmetric singlet doubles is not negligible in general. For instance, N_2 at equilibrium in a double-zeta basis has non-negligible dynamic correlations coming from the antisymmetric doubles. Neglecting these correlations results in the CCSD0 energy being too high not only at the dissociation limit but also at the equilibrium geometry.[127] Furthermore, Their recent efforts of incorporating antisymmetric singlet doubles with the frozen symmetric singlet doubles amplitudes suggest that an alternative route should be investigated.[133]

We would also like to mention externally corrected CCSD[134] which employs TQ obtained from external wavefunctions such as CASSCF,[135,136] valence-bond (VB),[137–139] broken-symmetry HF.[113,140,141] In particular CCSDQ', pioneered by Paldus, Piecuch and co-workers,[113,141] has similarities to the method to be discussed in this paper. In CCSDQ', one augments CCSD amplitudes equations with Q obtained from a cluster analysis of projection-after-variation PHF wavefunctions.[142] The resulting wavefunction is rigorously spin-pure, and it showed promising results on simple MR systems such as H_4 and H_8. In passing, we note that CCSDQ' (or CCDQ') is closely related to aforementioned ACPQ, the major difference being that CCSDQ' is not a self-contained method.

Two of us (D.W.S and M.H.G.) introduced coupled-cluster valence-bond theory singles and doubles (CCVB-SD) as a simple modification to RCCSD to describe strongly correlated *closed-shell* systems.[143] As opposed to completely removing certain quadratic terms from RCCSD or using external sources for higher excitations, CCVB-SD directly models Q with its D. The way it models Q originated from a simpler model, CCVB, which yields a spin-pure

wavefunction and can describe simultaneous multiple bond breaking at a cost dominated by integral transformations.[144–146] CCVB was formulated based on the recognition of a modified cluster expansion hidden in PHF. In this regard CCVB-SD is similar in spirit to ACPQ and CCSDQ'. The similarity between CCVB-SD and ACPQ was noticed in ref. 143. The key distinction is CCVB-SD is self-contained, unlike CCSDQ', and removes certain quadratic terms in RCCSD by solving modified amplitudes equations as opposed to discarding such terms *a priori*, as in ACPQ.

In CCVB-SD, a singlet doubly-excited configuration is constructed by pairing an occupied orbital with a virtual orbital and coupling two triplets out of such two pairs to form an overall singlet state. This is how CCVB encodes interpair correlations, and the remaining higher-order correlations enter through the aforementioned modified cluster expansion. CCVB-SD successfully combines advantages of RCCSD and CCVB: it preserves all the formal properties of RCCSD mentioned above and describes valence correlations correctly even near multiple bond dissociations. Another viewpoint is obtained by noting that CCVB generalizes PHF, removing the latter's size inconsistency, and CCVB-SD generalizes CCVB. Therefore, CCVB-SD is an effective combination of PHF and coupled cluster. The value of finding such a combination was emphasized in a recent paper.[147] We also note that CCVB-SD naturally contains the antisymmetric doubles that are discarded in CCSD0. When properly implemented, CCVB-SD should scale the same as does RCCSD, which is $n_{occ}^2 n_{vir}^4$. Its result for the triple-bond dissociation of N_2 in a minimal basis shows its ability to capture strong correlations in the valence space as it reaches the correct asymptote.[143]

The main objective of this paper is to provide detailed information about a new production-level implementation of CCVB-SD and discuss its applicability to systems of hundreds of strongly correlated electrons with an application to emergent many-electron correlations in oligoacenes,[22,23,148–157] which have been the focus of much recent attention. This paper is organised as follows: (1) we review and discuss the CCVB-SD wavefunction ansatz from a different angle than what is discussed in ref. 143, (2) we discuss the derivation of CCVB-

SD Λ-equation, (3) we illustrate how we implement the CCVB-SD T-amplitudes equation and Λ-equation solvers into a block-tensor based coupled-cluster code, and (4) we apply CCVB-SD to oligoacenes and discuss strong correlations in their ground state.

The Model

In CCVB-SD, the wavefunction ansatz is given through quadruples level as[143]

$$|\Psi\rangle = \left(\hat{\mathrm{I}} + \hat{\mathcal{T}}_1 + \frac{1}{2}\hat{\mathcal{T}}_1^2 + \hat{\mathcal{S}} + \frac{1}{6}\hat{\mathcal{T}}_1^3 + \frac{1}{2}\hat{\mathcal{S}}\hat{\mathcal{T}}_1^2 + \hat{\mathcal{S}}\hat{\mathcal{T}}_1 + \frac{1}{24}\hat{\mathcal{T}}_1^4 + \frac{1}{2}\hat{\mathcal{S}}^2 - \frac{1}{2}\hat{\mathrm{I}}_S\hat{\mathcal{Q}}^2\right)|\Phi_0\rangle, \quad (1)$$

where $|\Phi_0\rangle$ denotes a singlet reference, $\hat{\mathcal{T}}_1$ represents the singles operator, the doubles operator $\hat{\mathcal{S}}$ creates singlet doubly-excited configurations, the doubles operator $\hat{\mathcal{Q}}$ creates quintet doubly-excited configurations, and $\hat{\mathrm{I}}_S$ is a general singlet-subspace projection operator which can be written as a sum of outer products of orthonormal singlet states $\{|\Phi_\mu\rangle\}$,

$$\hat{\mathrm{I}}_S = |\Phi_0\rangle\langle\Phi_0| + \sum_{ia} |\Phi_i^a\rangle\langle\Phi_i^a| + \sum_{ijab} |\Phi_{ij}^{ab}\rangle\langle\Phi_{ij}^{ab}| + \cdots. \quad (2)$$

This ansatz includes full singles and doubles operators, and thus it is exact for isolated two-electron systems. The $\hat{\mathrm{I}}_S\hat{\mathcal{Q}}^2$ term represents an approximate connected quadruples contribution that plays a key role in capturing strong correlations in CCVB-SD.

Based on this wavefunction ansatz, the CCVB-SD energy and amplitudes equations follow

$$E = \langle\Phi_0| e^{-\hat{\mathcal{G}}}\mathcal{H}e^{\hat{\mathcal{G}}} |\Phi_0\rangle = \langle\Phi_0| \left(e^{-\hat{\mathcal{G}}}\hat{\mathcal{H}}e^{\hat{\mathcal{G}}} - \hat{\mathcal{H}}\,\hat{\mathrm{I}}_S\frac{1}{2}\hat{\mathcal{Q}}^2\right)|\Phi_0\rangle, \quad (3)$$

$$0 = \langle\Delta_\mu| \left(e^{-\hat{\mathcal{G}}}\hat{\mathcal{H}}e^{\hat{\mathcal{G}}} - \hat{\mathcal{H}}\,\hat{\mathrm{I}}_S\frac{1}{2}\hat{\mathcal{Q}}^2\right)|\Phi_0\rangle, \quad (4)$$

where the primary cluster operator $\hat{\mathcal{G}}$ is defined as

$$\hat{\mathcal{G}} = \hat{\mathcal{T}}_1 + \hat{\mathcal{S}}, \quad (5)$$

and $|\Delta_\mu\rangle$ represents an excited determinant in the spin-orbital basis including singly-excited ones $\left|\Delta_{i_{\sigma_1}}^{a_{\sigma_1}}\right\rangle$ and doubly-excited ones $\left|\Delta_{i_{\sigma_1} j_{\sigma_2}}^{a_{\sigma_1} b_{\sigma_2}}\right\rangle$. We note that in the second equality in Eq. (3) we used

$$\langle\Phi_0| \left(\hat{\mathcal{H}}\ \hat{\mathrm{I}}_S \frac{1}{2}\hat{\mathcal{Q}}^2\right) |\Phi_0\rangle = 0, \tag{6}$$

which is a consequence of the Slater rules. CCVB-SD formally includes other higher disconnected excitations beyond quadruples, but we only need up to quadruples for the purpose of solving the amplitude equations.

It is important to note that the amplitudes of $\hat{\mathcal{S}}$ parametrise the amplitudes of $\hat{\mathcal{Q}}$. This connection is most succinct if we use the following configurations for the singlet doubles subspace, indexed by spatial orbitals and grouped into 2 categories: $|^S\Phi_{ij}^{ab}\rangle$ and $|^A\Phi_{ij}^{ab}\rangle$ where the superscripts S and A denote symmetry and antisymmetry under the permutation of spatial orbital indices (i.e. i↔j, a↔b), respectively. This construction is based on the orthogonal spin-adapted 4-electron singlet configurations discussed extensively elsewhere.[128–131] As illustrated in Fig. 1, the symmetric state is constructed by taking two singlets from (ij) (a 2-particle geminal made from occupied levels i and j) and (ab) (a 2-particle geminal made from virtual levels a and b) to form a 4-electron singlet. The antisymmetric state, on the other hand, is built coupling two triplets from (ij) and (ab) to form an overall singlet.
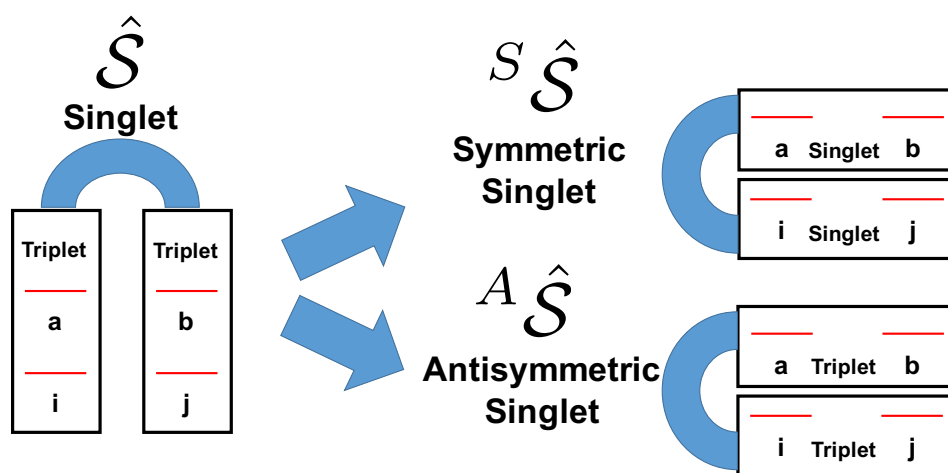

Figure 1: An illustration of the decomposition of singlet doubles space into antisymmetric and symmetric singlet parts.

In terms of excitations from a singlet reference $|\Phi_0\rangle$, the construction of $|^S\Phi_{ij}^{ab}\rangle$ and $|^A\Phi_{ij}^{ab}\rangle$ can be carried out using spin-adapted geminal (or pair) operators. The singlet annihilation operator $\hat{\sigma}_{pq}$ and the three triplet annihilation operators $(^{-1}\hat{\tau}_{pq},\ ^0\hat{\tau}_{pq},^1\hat{\tau}_{pq})$ for each M_S are defined as follows:

$$\hat{\sigma}_{pq} = \frac{1}{\sqrt{2}}\left(\hat{a}_{q_\beta}\hat{a}_{p_\alpha} + \hat{a}_{p_\beta}\hat{a}_{q_\alpha}\right), \tag{7}$$

$$^{-1}\hat{\tau}_{pq} = \hat{a}_{q_\beta}\hat{a}_{p_\beta}, \tag{8}$$

$$^0\hat{\tau}_{pq} = \frac{1}{\sqrt{2}}\left(\hat{a}_{q_\beta}\hat{a}_{p_\alpha} - \hat{a}_{p_\beta}\hat{a}_{q_\alpha}\right), \tag{9}$$

and

$$^1\hat{\tau}_{pq} = \hat{a}_{q_\alpha}\hat{a}_{p_\alpha}. \tag{10}$$

Applying these operators to $|\Phi_0\rangle$, $|^S\Phi_{ij}^{ab}\rangle$ and $|^A\Phi_{ij}^{ab}\rangle$ follow

$$
\begin{aligned}
|^S\Phi_{ij}^{ab}\rangle &= {}^{ss}\hat{\Sigma}_{ij}^{ab}|\Phi_0\rangle \\
&= \frac{1}{2}\left(|\Delta_{i_\beta j_\alpha}^{b_\beta a_\alpha}\rangle + |\Delta_{i_\alpha j_\beta}^{b_\alpha a_\beta}\rangle + |\Delta_{i_\beta j_\alpha}^{a_\beta b_\alpha}\rangle + |\Delta_{i_\alpha j_\beta}^{a_\alpha b_\beta}\rangle\right),
\end{aligned}
\tag{11}
$$

and

$$
\begin{aligned}
|^A\Phi_{ij}^{ab}\rangle &= {}^{tt}\hat{\Sigma}_{ij}^{ab}|\Phi_0\rangle \\
&= \frac{1}{\sqrt{12}}\left(|\Delta_{i_\beta j_\alpha}^{b_\beta a_\alpha}\rangle + |\Delta_{i_\alpha j_\beta}^{b_\alpha a_\beta}\rangle - |\Delta_{i_\beta j_\alpha}^{a_\beta b_\alpha}\rangle - |\Delta_{i_\alpha j_\beta}^{a_\alpha b_\beta}\rangle - 2|\Delta_{i_\beta j_\beta}^{a_\beta b_\beta}\rangle - 2|\Delta_{i_\alpha j_\alpha}^{a_\alpha b_\alpha}\rangle\right),
\end{aligned}
\tag{12}
$$

where

$$^{ss}\hat{\Sigma}_{ij}^{ab} = \hat{\sigma}_{ab}^\dagger\hat{\sigma}_{ij}, \tag{13}$$

and

$$^{tt}\hat{\Sigma}_{ij}^{ab} = \frac{1}{\sqrt{3}}\left(-^0\hat{\tau}_{ab}^\dagger\,{}^0\hat{\tau}_{ij} - {}^{-1}\hat{\tau}_{ab}^\dagger\,{}^{-1}\hat{\tau}_{ij} - {}^1\hat{\tau}_{ab}^\dagger\,{}^1\hat{\tau}_{ij}\right). \tag{14}$$

In the case of $|^S\Phi_{ij}^{ab}\rangle$, $\hat{\sigma}_{ij}$ removes a singlet from $|\Phi_0\rangle$ and in its place creates another singlet with $\hat{\sigma}_{ab}^\dagger$. Unsurprisingly, the result is a doubly-substituted singlet configuration. Construct-

ing $|^A\Phi_{ij}^{ab}\rangle$ is similar except that we must ensure that the resulting configuration is singlet. For example, $^0\hat{\tau}_{ij}$ removes a triplet from the reference and replaces it with another triplet via $^0\hat{\tau}_{ab}^\dagger$, but if we had stopped there, the configuration would still have a quintet component. In any case, the underlying concept in this viewpoint of the singlet doubles space is that we are removing two electrons of a given spin from the reference and replacing them with two electrons of the same spin. In passing, we note that this construction verifies the earlier assertion about the permutation symmetry of the two states as

$$|^S\Phi_{ij}^{ab}\rangle = |^S\Phi_{ij}^{ba}\rangle = |^S\Phi_{ji}^{ab}\rangle = |^S\Phi_{ji}^{ba}\rangle, \tag{15}$$

and

$$|^A\Phi_{ij}^{ab}\rangle = -|^A\Phi_{ij}^{ba}\rangle = -|^A\Phi_{ji}^{ab}\rangle = |^A\Phi_{ji}^{ba}\rangle. \tag{16}$$

We also note that Eq. (11) is not normalised for cases with repeated indices, but it is consistent with our definition of $^S\hat{S}$ shown below. With these, the singlet doubles operator $\hat{S}$ thus separates into two orbital-invariant pieces

$$\hat{S} = {}^S\hat{S} + {}^A\hat{S}, \tag{17}$$

where the symmetric part of $\hat{S}$ is

$$^S\hat{S} = \frac{1}{4}\sum_{ijab} {}^S S_{ij}^{ab}\, {}^{ss}\hat{\Sigma}_{ij}^{ab}, \tag{18}$$

and the antisymmetric part of $\hat{S}$ is

$$^A\hat{S} = \frac{1}{4}\sum_{ijab} {}^A S_{ij}^{ab}\, {}^{tt}\hat{\Sigma}_{ij}^{ab}. \tag{19}$$

$^S S_{ij}^{ab}$ and $^A S_{ij}^{ab}$ have the same index symmetry as the corresponding substitution operators (i.e. they follow the same symmetry as Eq. (15) and Eq. (16), respectively). These two

sets of amplitudes constitute two tensors $^S\mathbf{S}$ and $^A\mathbf{S}$, each of size $n_{\mathrm{occ}}^2 n_{\mathrm{vir}}^2$. Because the amplitude indices are for spatial orbitals, the tensors will be referred to as being "spinless". In contrast to this, tensors indexed with spin orbitals will be referred to as "spinful" tensors. For completeness, we write $\hat{\mathcal{S}}$ in terms of spin blocks of its spinful counterpart $\hat{s}$ as in

$$\hat{\mathcal{S}} = \frac{1}{4} \sum_{ijab} s_{i_\alpha j_\alpha}^{a_\alpha b_\alpha} \left(\hat{a}_{a_\alpha}^\dagger \hat{a}_{b_\alpha}^\dagger \hat{a}_{j_\alpha} \hat{a}_{i_\alpha} + \hat{a}_{a_\beta}^\dagger \hat{a}_{b_\beta}^\dagger \hat{a}_{j_\beta} \hat{a}_{i_\beta} \right) + \sum_{ijab} s_{i_\alpha j_\beta}^{a_\alpha b_\beta} \hat{a}_{a_\alpha}^\dagger \hat{a}_{b_\beta}^\dagger \hat{a}_{j_\beta} \hat{a}_{i_\alpha}, \tag{20}$$

where the summations run over spatial orbitals, the first term denotes the same spin block of $\hat{s}$ and the second term is the opposite spin block of $\hat{s}$.

When acting on $|\Phi_0\rangle$, $\hat{\mathcal{Q}}$ creates a linear combination of quintet configurations. Because the maximum spin for four electrons is quintet, it is clear that each quintet double should be obtained by removing a triplet from the reference and replacing it with another triplet. We have

$$\hat{\mathcal{Q}} = \frac{1}{4} \sum_{ijab} Q_{ij}^{ab} \, ^{tt}\hat{\kappa}_{ij}^{ab}, \tag{21}$$

where

$$^{tt}\hat{\kappa}_{ij}^{ab} = \frac{1}{\sqrt{6}} \left(-2\, ^0\hat{\tau}_{ab}^\dagger\, ^0\hat{\tau}_{ij} + \, ^{-1}\hat{\tau}_{ab}^\dagger\, ^{-1}\hat{\tau}_{ij} + \, ^1\hat{\tau}_{ab}^\dagger\, ^1\hat{\tau}_{ij} \right), \tag{22}$$

and $\mathbf{Q}$ is another spinless antisymmetric tensor of size $n_{\mathrm{occ}}^2 n_{\mathrm{vir}}^2$. The action of $^{tt}\hat{\kappa}_{ij}^{ab}$ creates a quintet configuration as in

$$|^Q\Phi_{ij}^{ab}\rangle = \, ^{tt}\hat{\kappa}_{ij}^{ab} |\Phi_0\rangle \tag{23}$$

$$= \frac{1}{\sqrt{6}} \left(|\Delta_{i_\beta j_\alpha}^{b_\beta a_\alpha}\rangle + |\Delta_{i_\alpha j_\beta}^{b_\alpha a_\beta}\rangle - |\Delta_{i_\beta j_\alpha}^{a_\beta b_\alpha}\rangle - |\Delta_{i_\alpha j_\beta}^{a_\alpha b_\beta}\rangle + |\Delta_{i_\beta j_\beta}^{a_\beta b_\beta}\rangle + |\Delta_{i_\alpha j_\alpha}^{a_\alpha b_\alpha}\rangle \right). \tag{24}$$

We can now describe the correspondence between $\mathbf{S}$ and $\mathbf{Q}$, which is given by

$$Q_{ij}^{ab} = -2\, ^A S_{ij}^{ab}. \tag{25}$$

This indicates that $\mathbf{Q}$ is independent of $^S\mathbf{S}$ and parametrised by $^A\mathbf{S}$. This is intuitive given

that $^A\mathbf{S}$ and $\mathbf{Q}$ have the same permutational symmetry in the spatial orbitals, or alternatively they are both obtained by substituting triplets within the reference. The detailed proof of Eq. (25) is available in Appendix of this article.

The physical meaning of $^S\hat{\mathcal{S}}$ and $^A\hat{\mathcal{S}}$ may be better understood in the language of valence bond theory.[158] $^S\hat{\mathcal{S}}$ contains perfect-pairing (PP)[159] terms which are important pieces of strong correlations that describe intrapair correlations. In addition to PP terms, it also has important interpair correlations such as ionic excitations between two pairs. On the other hand, $^A\hat{\mathcal{S}}$ corresponds to interpair correlations which are not captured by $^S\hat{\mathcal{S}}$ but are important to describe polyradical character of systems. $^A\mathbf{S}$ parametrises quadruples in a different way than they are parametrised in RCCSD. If $^A\mathbf{S}$ is small, then $\mathbf{Q}$ is small and so is the difference between the CCVB-SD and RCCSD results. In this sense, CCVB-SD theory asserts that $^A\mathbf{S}$ is the operative element (at least for the doubles) in RCCSD's failure to correctly describe strong correlations. This also stands in contrast to the CCSD0 method[127] which removes $^A\mathbf{S}$ or $^A\hat{\mathcal{S}}$ entirely.

CCVB-SD Lagrangian and $\Lambda-$equation

Following Eq. (3) and (4), we establish the CCVB-SD Lagrangian defined as

$$\mathcal{L}(\hat{\mathcal{T}}_1, \hat{\mathcal{S}}, \hat{\Lambda}) = \langle \Phi_0 | \left(\hat{I} + \hat{\Lambda} \right) \left(e^{-\hat{\mathcal{G}}} \hat{\mathcal{H}} e^{\hat{\mathcal{G}}} - \hat{\mathcal{H}} \ \hat{I}_S \frac{1}{2} \hat{\mathcal{Q}}^2 \right) | \Phi_0 \rangle , \qquad (26)$$

where $\hat{\Lambda}$, a deexcitation operator multiplied by Lagrange's multipliers, is defined as

$$\begin{aligned} \hat{\Lambda} &= \hat{\Lambda}_1 + \hat{\Lambda}_2 \\ &= \sum_{ia} \Lambda_i^a \hat{E}_a^i + \frac{1}{2} \sum_{ijab} \Lambda_{ij}^{ab} \hat{E}_a^i \hat{E}_b^j, \end{aligned} \qquad (27)$$

with the unitary-group generator

$$\hat{E}_i^a = \hat{a}_{a_\alpha}^\dagger \hat{a}_{i_\alpha} + \hat{a}_{a_\beta}^\dagger \hat{a}_{i_\beta}. \tag{28}$$

 If we did not have the quintet contribution, we would have exactly the same Lagrangian as RCCSD. Finding a stationary point of $\mathcal{L}$ with respect to the variations of t_i^a, $^S S_{ij}^{ab}$, and $^A S_{ij}^{ab}$ yields the CCVB-SD Λ-equation. For the singles equations, it can be easily shown that the resulting equation is essentially identical to the one for RCCSD with the cluster operator $\hat{\mathcal{G}}$.[160] Below we shall discuss how the doubles equations differ from the usual RCCSD Λ-equation.

From Eq. (25),

$$\frac{\partial \hat{\mathcal{Q}}}{\partial\, ^A S_{ij}^{ab}} = -2\, ^{tt}\hat{\kappa}_{ij}^{ab}, \tag{29}$$

and the quintet contribution for the Λ-equation follows

$$2 \langle\Phi_0| \left(\hat{\mathrm{I}} + \hat{\Lambda}\right) \left(\hat{\mathcal{H}}\, \hat{\mathrm{I}}_S\, {}^{tt}\hat{\kappa}_{ij}^{ab}\hat{\mathcal{Q}}\right) |\Phi_0\rangle = 2 \langle\Phi_0| \hat{\Lambda}_2\hat{\mathcal{H}}\, \hat{\mathrm{I}}_S\, {}^{tt}\hat{\kappa}_{ij}^{ab}\hat{\mathcal{Q}} |\Phi_0\rangle . \tag{30}$$

Using

$$\langle\Phi_0| \left(\hat{\mathrm{I}} + \hat{\Lambda}_2\right) e^{-\hat{\mathcal{Q}}}[\hat{\mathcal{H}}, {}^{tt}\hat{\kappa}_{ij}^{ab}]e^{\hat{\mathcal{Q}}} |\Phi_0\rangle = \langle\Phi_0| \hat{\Lambda}_2\hat{\mathcal{H}}\, \hat{\mathrm{I}}_S\, {}^{tt}\hat{\kappa}_{ij}^{ab}\hat{\mathcal{Q}} |\Phi_0\rangle , \tag{31}$$

the quintet contribution can be reshaped similarly to the RCCD Λ-equation expression with the doubles operator being $\hat{\mathcal{Q}}$.

Using this, the CCVB-SD Λ-equation in a spatial-orbital form for each variation with

respect to ${}^S S_{ij}^{ab}$ and ${}^A S_{ij}^{ab}$ is written as

$$\frac{\partial \mathcal{L}}{\partial {}^S S_{ij}^{ab}} = 0 \rightarrow \langle \Phi_0 | \left(\hat{\mathbb{I}} + \hat{\Lambda} \right) e^{-\hat{\mathcal{G}}} \left[\hat{\mathcal{H}}, {}^{ss}\hat{\Sigma}_{ij}^{ab} \right] e^{\hat{\mathcal{G}}} | \Phi_0 \rangle = 0, \tag{32}$$

$$\frac{\partial \mathcal{L}}{\partial {}^A S_{ij}^{ab}} = 0 \rightarrow \langle \Phi_0 | \left(\hat{\mathbb{I}} + \hat{\Lambda} \right) e^{-\hat{\mathcal{G}}} \left[\hat{\mathcal{H}}, {}^{tt}\hat{\Sigma}_{ij}^{ab} \right] e^{\hat{\mathcal{G}}} | \Phi_0 \rangle \tag{33}$$

$$+ 2 \langle \Phi_0 | \left(\hat{\mathbb{I}} + \hat{\Lambda}_2 \right) e^{-\hat{\mathcal{Q}}} [\hat{\mathcal{H}}, {}^{tt}\hat{\kappa}_{ij}^{ab}] e^{\hat{\mathcal{Q}}} | \Phi_0 \rangle = 0.$$

This can be further simplified to more familiar forms[160],

$$\langle \Phi_0 | \left(\bar{\mathcal{H}}^{\hat{\mathcal{G}}} + \left[\hat{\Lambda}, \bar{\mathcal{H}}^{\hat{\mathcal{G}}} \right] + \sum_{kc} \bar{\mathcal{H}}^{\hat{\mathcal{G}}} | \Phi_k^c \rangle \langle \Phi_k^c | \hat{\Lambda}_1 \right) | {}^S \Phi_{ij}^{ab} \rangle = 0, \tag{34}$$

$$\langle \Phi_0 | \left(\bar{\mathcal{H}}^{\hat{\mathcal{G}}} + \left[\hat{\Lambda}, \bar{\mathcal{H}}^{\hat{\mathcal{G}}} \right] + \sum_{kc} \bar{\mathcal{H}}^{\hat{\mathcal{G}}} | \Phi_k^c \rangle \langle \Phi_k^c | \hat{\Lambda}_1 \right) | {}^A \Phi_{ij}^{ab} \rangle$$

$$+ 2 \langle \Phi_0 | \left(\bar{\mathcal{H}}^{\hat{\mathcal{Q}}} + \left[\hat{\Lambda}_2, \bar{\mathcal{H}}^{\hat{\mathcal{Q}}} \right] \right) | {}^Q \Phi_{ij}^{ab} \rangle = 0, \tag{35}$$

where we define

$$\bar{\mathcal{H}}^{\hat{\mathcal{O}}} = e^{-\hat{\mathcal{O}}} \hat{\mathcal{H}} e^{\hat{\mathcal{O}}}. \tag{36}$$

Eq. (34) can be used to update the symmetric part of Λ_{ij}^{ab} (i.e. ${}^S \Lambda_{ij}^{ab}$) whilst Eq. (35) can be used to update the antisymmetric part of Λ_{ij}^{ab} (i.e. ${}^A \Lambda_{ij}^{ab}$) .

Unrelaxed PDMs

It can be verified that the expression of the CCVB-SD one-particle density matrix (1PDM) is identical to that of RCCSD.[160] On the other hand, the expression for the two-particle density matrix (2PDM) has an extra term associated with $\hat{\mathcal{Q}}$. To see this, we define a spin-orbital tensor of size $2(n_{\text{occ}} + n_{\text{vir}})^4$ (having both same-spin and opposite-spin blocks) that

represents the CCVB-SD unrelaxed 2PDM:

$$\xi^{p_{\sigma_1} q_{\sigma_2}}_{r_{\sigma_1} s_{\sigma_2}} = \langle \Phi_0 | \, (\hat{I} + \hat{\Lambda}) \left(e^{-\hat{\mathcal{G}}} (\hat{a}^{\dagger}_{p_{\sigma_1}} \hat{a}^{\dagger}_{q_{\sigma_2}} \hat{a}_{s_{\sigma_2}} \hat{a}_{r_{\sigma_1}}) e^{\hat{\mathcal{G}}} - \frac{1}{2} (\hat{a}^{\dagger}_{p_{\sigma_1}} \hat{a}^{\dagger}_{q_{\sigma_2}} \hat{a}_{s_{\sigma_2}} \hat{a}_{r_{\sigma_1}}) \hat{I}_S \hat{\mathcal{Q}}^2 \right) |\Phi_0\rangle \tag{37}$$

$$= {}^{\hat{\mathcal{G}}}\xi^{p_{\sigma_1} q_{\sigma_2}}_{r_{\sigma_1} s_{\sigma_2}} + {}^{\hat{\mathcal{Q}}}\xi^{p_{\sigma_1} q_{\sigma_2}}_{r_{\sigma_1} s_{\sigma_2}}, \tag{38}$$

where

$$ {}^{\hat{\mathcal{G}}}\xi^{p_{\sigma_1} q_{\sigma_2}}_{r_{\sigma_1} s_{\sigma_2}} = \langle \Phi_0 | \, (\hat{I} + \hat{\Lambda}) e^{-\hat{\mathcal{G}}} (\hat{a}^{\dagger}_{p_{\sigma_1}} \hat{a}^{\dagger}_{q_{\sigma_2}} \hat{a}_{s_{\sigma_2}} \hat{a}_{r_{\sigma_1}}) e^{\hat{\mathcal{G}}} |\Phi_0\rangle \,, \tag{39}$$

and

$$ {}^{\hat{\mathcal{Q}}}\xi^{p_{\sigma_1} q_{\sigma_2}}_{r_{\sigma_1} s_{\sigma_2}} = -\frac{1}{2} \langle \Phi_0 | \, (\hat{I} + \hat{\Lambda}) (\hat{a}^{\dagger}_{p_{\sigma_1}} \hat{a}^{\dagger}_{q_{\sigma_2}} \hat{a}_{s_{\sigma_2}} \hat{a}_{r_{\sigma_1}}) \hat{I}_S \hat{\mathcal{Q}}^2 |\Phi_0\rangle \,. \tag{40}$$

${}^{\hat{\mathcal{G}}}\xi$ is the RCCSD contribution with the cluster operator $\hat{\mathcal{G}}$, and ${}^{\hat{\mathcal{Q}}}\xi$ is an extra term coming from $\hat{\mathcal{Q}}$. It is clear that the second term contributes to only OOVV blocks (i.e. $\xi^{i_{\sigma_1} j_{\sigma_2}}_{a_{\sigma_1} b_{\sigma_2}}$) because $\hat{\mathcal{Q}}^2$ produces quadruply excited configurations. We then use a similar trick used in Eq. (31) to write the extra term in the following form:

$$ {}^{\hat{\mathcal{Q}}}\xi^{p_{\sigma_1} q_{\sigma_2}}_{r_{\sigma_1} s_{\sigma_2}} = - \langle \Phi_0 | \, (\hat{I} + \hat{\Lambda}_2) e^{-\hat{\mathcal{Q}}} (\hat{a}^{\dagger}_{i_{\sigma_1}} \hat{a}^{\dagger}_{j_{\sigma_2}} \hat{a}_{b_{\sigma_2}} \hat{a}_{a_{\sigma_1}}) \hat{I}_S e^{\hat{\mathcal{Q}}} |\Phi_0\rangle \,. \tag{41}$$

Having these unrelaxed PDMs allows for computing unrelaxed one-electron and two-electron properties.

As the formation of relaxed PDMs (i.e. response equations) for CCVB-SD remains unchanged from RCCSD,[160] all the relaxed properties of CCVB-SD are computed by usual ways as is done for RCCSD. The analytical gradients can be readily implemented in general coupled-cluster codes.

Block-Tensor Implementation of CCVB-SD

In this section, we use uppercase letters such as S, ${}^S S$, ${}^A S$, Q, Λ, ${}^S \Lambda$, and ${}^A \Lambda$ to indicate spinless tensors or operators as before, and lowercase letters such as s, q, μ, ν, λ, ρ, ζ, and

ξ are used for spinful tensors, i.e. ones with spin-orbital indices.

Tensorial Properties of Doubles Operators

In a spin-orbital based implementation, $\hat{\mathcal{S}}$ is represented by a set of amplitudes $s_{i_{\sigma_1} j_{\sigma_2}}^{a_{\sigma_1} b_{\sigma_2}}$ as shown in Eq. (20). With this, we can extract $^A\mathbf{S}$:

$$
^A S_{ij}^{ab} = \frac{1}{\sqrt{12}} \left(s_{i_\beta j_\alpha}^{b_\beta a_\alpha} + s_{i_\alpha j_\beta}^{b_\alpha a_\beta} - s_{i_\beta j_\alpha}^{a_\beta b_\alpha} - s_{i_\alpha j_\beta}^{a_\alpha b_\beta} - 2 s_{i_\beta j_\beta}^{a_\beta b_\beta} - 2 s_{i_\alpha j_\alpha}^{a_\alpha b_\alpha} \right). \tag{42}
$$

This form, however, poses a little challenge when embedded into block-tensor based codes as accessing individual elements of tensors will be highly inefficient. Manipulating such equations in terms of block tensors instead of individual elements is thus valuable.

Q-Chem's[161] coupled-cluster code, ccman2, extensively employs the block tensors implemented in a general tensor library called libtensor.[162] In libtensor, any doubles amplitudes of the form $o_{i_{\sigma_1} j_{\sigma_2}}^{a_{\sigma_1} b_{\sigma_2}}$ are stored only with non-zero, symmetry-unique blocks, called canonical blocks. For instance, when unrestricted orbitals are used there are three canonical blocks (i.e. $(\alpha\alpha\alpha\alpha)$, $(\beta\beta\beta\beta)$, $(\alpha\beta\alpha\beta)$) out of the total six blocks illustrated in Figure 2. In the case of restricted orbitals and closed-shell molecules (or more generally singlet operators), one needs only opposite-spin blocks (i.e. $(\alpha\beta\alpha\beta)$) to form the entire tensor. This is because restricted orbitals imply the $\alpha \leftrightarrow \beta$ symmetry and for singlet operators same-spin blocks can be obtained by antisymmetrising opposite-spin blocks.

This can be seen from the form of a singlet configuration $|\Phi\rangle = \hat{\mathcal{S}}|\Phi_0\rangle$. The projection of this state onto the same-spin space is simply obtained as

$$
s_{i_\alpha j_\alpha}^{a_\alpha b_\alpha} = \langle \Delta_{i_\alpha j_\alpha}^{a_\alpha b_\alpha} | \hat{\mathcal{S}} | \Phi_0 \rangle = -\frac{1}{\sqrt{3}} {}^A S_{ij}^{ab}. \tag{43}
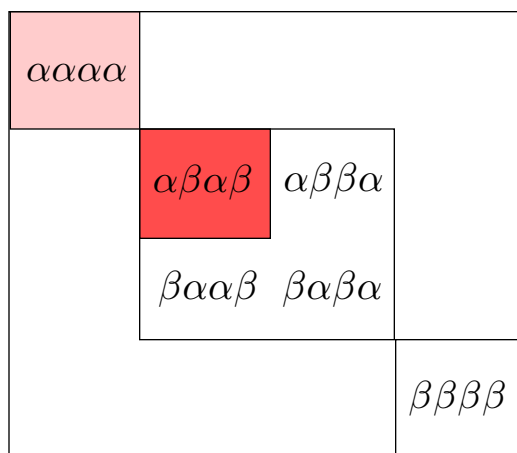$$

Figure 2: The data structure of block tensors of order 4. Colored blocks are only canonical blocks for tensors with restricted orbitals, and $(\alpha\alpha\alpha\alpha)$ block can be obtained from $(\alpha\beta\alpha\beta)$ block in the case of singlet operators.

Similarly, the opposite-spin projection is

$$s_{i_\alpha j_\beta}^{a_\alpha b_\beta} = \langle \Delta_{i_\alpha j_\beta}^{a_\alpha b_\beta} | \hat{\mathcal{S}} | \Phi_0 \rangle = \frac{1}{2} {}^S S_{ij}^{ab} - \frac{1}{\sqrt{12}} {}^A S_{ij}^{ab}, \tag{44}$$

$$s_{i_\alpha j_\beta}^{b_\alpha a_\beta} = \langle \Delta_{i_\alpha j_\beta}^{b_\alpha a_\beta} | \hat{\mathcal{S}} | \Phi_0 \rangle = \frac{1}{2} {}^S S_{ij}^{ab} + \frac{1}{\sqrt{12}} {}^A S_{ij}^{ab}. \tag{45}$$

This shows that for any combination of (i, j) and (a, b) including $i = j$ or $a = b$

$$s_{i_\alpha j_\alpha}^{a_\alpha b_\alpha} = s_{i_\alpha j_\beta}^{a_\alpha b_\beta} - s_{i_\alpha j_\beta}^{b_\alpha a_\beta}. \tag{46}$$

Similarly, one can show

$$s_{i_\alpha j_\alpha}^{a_\alpha b_\alpha} = \frac{1}{2} \left(s_{i_\alpha j_\beta}^{a_\alpha b_\beta} - s_{i_\alpha j_\beta}^{b_\alpha a_\beta} + s_{j_\alpha i_\beta}^{b_\alpha a_\beta} - s_{j_\alpha i_\beta}^{a_\alpha b_\beta} \right). \tag{47}$$

As long as restricted orbitals are employed, both Eq. (46) and Eq. (47) are identical. The latter is preferred for the purpose of demonstration because it is easier to see the full antisymmetrisation with respect to permuting either occupied orbitals or virtual orbitals.

Symbolically, we write Eq. (47) as

$$\texttt{SS(s)} = \frac{1}{2} \, \texttt{asymm}_\texttt{O} \, [\, \texttt{asymm}_\texttt{V} \, [\, \texttt{OS(s)} \,]\,], \tag{48}$$

where $\texttt{SS}(\cdot)$ denotes the same-spin block of a given tensor as in

$$\texttt{SS(s)}\,_{ij}^{ab} = s_{i_\alpha j_\alpha}^{a_\alpha b_\alpha}, \tag{49}$$

$\texttt{OS}(\cdot)$ denotes the opposite-spin block of a given tensor as in

$$\texttt{OS(s)}\,_{ij}^{ab} = s_{i_\alpha j_\beta}^{a_\alpha b_\beta}, \tag{50}$$

and $\texttt{asymm}_\texttt{O}[\cdot]$ and $\texttt{asymm}_\texttt{V}[\cdot]$ perform antisymmetrisation of a given tensor over occupied and virtual spatial indices, respectively. Similarly, we define symmetrisation of a given tensor as $\texttt{symm}_\texttt{O}[\cdot]$ and $\texttt{symm}_\texttt{V}[\cdot]$ over occupied and virtual spatial indices, respectively. In passing, we note that Eq. (43) implies that the spinless antisymmetric part of a singlet tensor is obtained simply scaling the same-spin component of the corresponding singlet spinful tensor. This is again in the symbolic form:

$$^\texttt{A}\texttt{S} = -\sqrt{3} \; \texttt{SS(s)}. \tag{51}$$

We then illustrate the tensorial properties of $\mathbf{Q}$ which will be useful to derive block-tensor equations. It can be read from Eq. (24) that (similarly to Eq. (43))

$$\texttt{SS(q)} = \frac{1}{\sqrt{6}} \, \texttt{Q}. \tag{52}$$

and $(\alpha\alpha\alpha\alpha)$ and $(\beta\beta\beta\beta)$ blocks of $\mathbf{q}$ are identical. Combining this with Eq. (25) and Eq. (51), we arrive at

$$\texttt{SS(q)} = \frac{-2}{\sqrt{6}} \, ^\texttt{A}\texttt{S} = \sqrt{2} \; \texttt{SS(s)}. \tag{53}$$

This shows how the same-spin block of the spinful tensor $\mathbf{q}$ is related to the same-spin block

of a singlet tensor $\mathbf{s}$. Also, the opposite spin-block of $\mathbf{q}$ is

$$\mathtt{OS\,(q)} = -\ \mathtt{SS\,(q)}, \tag{54}$$

and this contrasts with Eq. (48), which manifests a different tensorial property of singlet and quintet tensors.

T-Amplitude Solver

The singles equation is identical to RCCSD with the doubles operator $\hat{\mathcal{G}}$, so we will focus on solving the doubles equation. Based on the properties of the doubles operators appearing in CCVB-SD discussed above, CCVB-SD can be efficiently implemented in a block-tensor based coupled cluster codes. The CCVB-SD amplitude equation reads

$$\rho_{i_{\sigma_1} j_{\sigma_2}}^{a_{\sigma_1} b_{\sigma_2}}(\hat{\mathcal{G}}) = \mu_{i_{\sigma_1} j_{\sigma_2}}^{a_{\sigma_1} b_{\sigma_2}}(\hat{\mathcal{G}}) - \left(\nu_{i_{\sigma_1} j_{\sigma_2}}^{a_{\sigma_1} b_{\sigma_2}}(\hat{\mathcal{Q}}) - \langle a_{\sigma_1} b_{\sigma_2} \,\|\, i_{\sigma_1} j_{\sigma_2} \rangle \right) = 0, \tag{55}$$

where we define

$$\mu_{i_{\sigma_1} j_{\sigma_2}}^{a_{\sigma_1} b_{\sigma_2}}(\hat{\mathcal{O}}) = \left\langle \Delta_{i_{\sigma_1} j_{\sigma_2}}^{a_{\sigma_1} b_{\sigma_2}} \left| \bar{\mathcal{H}}^{\hat{\mathcal{O}}} \right| \Phi_0 \right\rangle, \tag{56}$$

and

$$\nu_{i_{\sigma_1} j_{\sigma_2}}^{a_{\sigma_1} b_{\sigma_2}}(\hat{\mathcal{O}}) = \left\langle \Delta_{i_{\sigma_1} j_{\sigma_2}}^{a_{\sigma_1} b_{\sigma_2}} \left| \hat{\mathbf{I}}_S \bar{\mathcal{H}}^{\hat{\mathcal{O}}} \right| \Phi_0 \right\rangle. \tag{57}$$

$\mu(\hat{\mathcal{O}})$ can be obtained easily with any existing coupled-cluster codes whereas computing $\nu(\hat{\mathcal{O}})$ is not as straightforward. Below we illustrate how to solve this amplitudes equation with details on computing $\nu(\hat{\mathcal{Q}})$ from $\mu(\hat{\mathcal{Q}})$:

1. Perform the block-tensor operation demonstrated in Eq. (53) based on $\mathbf{s}$ either from the previous iteration or an initial guess. This gives $\mathtt{SS\,(q)}$ and then performing the operation in Eq. (54) yields the full $\mathbf{q}$ tensor.

2. Form $\mu(\hat{\mathcal{Q}})$ defined in Eq. (56). This can be achieved with any standard coupled-

cluster codes.

3. $\nu(\hat{\mathcal{Q}})$ is obtained through a spin-projection of $\mu(\hat{\mathcal{Q}})$ onto a 4-electron singlet subspace. Since $\nu(\hat{\mathcal{Q}})$ is strictly a singlet, we can utilize the tensorial properties of general singlet tensors discussed above. The upshot is that we only need to obtain $\mathtt{OS}(\nu(\hat{\mathcal{Q}}))$ and $\mathtt{SS}(\nu(\hat{\mathcal{Q}}))$ will be obtained using Eq. (48). For the sake of simplicity, we write μ and ν to indicate $\mu(\hat{\mathcal{Q}})$ and $\nu(\hat{\mathcal{Q}})$, respectively.

The element-wise definition of ν is well described in the appendix of ref. 143, which can be further simplified to

$$
\begin{aligned}
\nu^{a_\alpha b_\beta}_{i_\alpha j_\beta} &= \frac{1}{6}\left(\mu^{b_\beta a_\alpha}_{i_\beta j_\alpha} + \mu^{b_\alpha a_\beta}_{i_\alpha j_\beta} + 2\mu^{a_\beta b_\alpha}_{i_\beta j_\alpha} + 2\mu^{a_\alpha b_\beta}_{i_\alpha j_\beta} + \mu^{a_\beta b_\beta}_{i_\beta j_\beta} + \mu^{a_\alpha b_\alpha}_{i_\alpha j_\alpha}\right) \\
&= \frac{1}{3}\left(\mu^{b_\alpha a_\beta}_{i_\alpha j_\beta} + 2\mu^{a_\alpha b_\beta}_{i_\alpha j_\beta} + \mu^{a_\alpha b_\alpha}_{i_\alpha j_\alpha}\right),
\end{aligned}
\tag{58}
$$

where we used $\mu^{a_\alpha b_\beta}_{i_\alpha j_\beta} = \mu^{a_\beta b_\alpha}_{i_\beta j_\alpha}$. We then write this in a block-tensor form:

$$
\mathtt{OS}(\nu) = \frac{1}{3}\left(\mathtt{OS}(\mu) + \mathtt{symm_V}[\mathtt{OS}(\mu)] + \mathtt{SS}(\mu)\right).
\tag{59}
$$

The same-spin blocks are obtained using Eq. (48). In passing, we note that Eq. (58) gives a correct singlet tensor even when there are repeated indices. One can verify that this single operation yields all the spin-projected opposite-spin blocks of the tensor described in the appendix of ref. 143.

After evaluating $\rho(\hat{\mathcal{G}})$, a standard Jacobi iteration along with Pulay's direct inversion of the iterative subspace (DIIS)[163] can be used to solve for the amplitudes. This completes the implementation of the CCVB-SD T-amplitude solver. The computational cost of CCVB-SD has a larger prefactor (roughly twice larger) than RCCSD due to the need for constructing $\nu(\hat{\mathcal{Q}})$. As its asymptotic scaling is the same as RCCSD ($n^2_{\mathrm{occ}} n^4_{\mathrm{vir}}$), this is considered a minor drawback. More detailed information on the performance of this implementation is available in the applications discussed later.

Λ-Equation Solver

We define a general spin-orbital tensor γ that can be readily computed in usual coupled cluster programs as follows,

$$\gamma_{i_{\sigma_1} j_{\sigma_2}}^{a_{\sigma_1} b_{\sigma_2}}(\hat{\mathcal{O}}) = \langle \Phi_0 | \left(\bar{\mathcal{H}}^{\hat{\mathcal{O}}} + \left[\hat{\Lambda}, \bar{\mathcal{H}}^{\hat{\mathcal{O}}} \right] + \sum_{kc} \bar{\mathcal{H}}^{\hat{\mathcal{O}}} | \Phi_k^c \rangle \langle \Phi_k^c | \hat{\Lambda}_1 \right) \left| \Delta_{i_{\sigma_1} j_{\sigma_2}}^{a_{\sigma_1} b_{\sigma_2}} \right\rangle. \tag{60}$$

Using this tensor and Eq. (11), Eq. (34) can be achieved by

$$\frac{1}{2} \, \texttt{symm}_V \, [\, \texttt{symm}_O \, [\, \texttt{OS} \, (\gamma(\hat{\mathcal{G}})) \,] \,], \tag{61}$$

whereas with Eq. (12) and Eq. (24), Eq. (35) can be written as

$$\frac{1}{\sqrt{3}} \left(-\frac{1}{2} \, \texttt{asymm}_V \, [\, \texttt{asymm}_O \, [\, \texttt{OS} \, (\gamma(\hat{\mathcal{G}})) \,] - 2 \, \texttt{SS} \, (\gamma(\hat{\mathcal{G}})) \right)$$
$$+ \frac{4}{\sqrt{6}} \left(-\frac{1}{2} \, \texttt{asymm}_V \, [\, \texttt{asymm}_O \, [\, \texttt{OS} \, (\gamma(\hat{\mathcal{Q}})) \,] + \texttt{SS} \, (\gamma(\hat{\mathcal{Q}})) \right). \tag{62}$$

Combining these with Eq. (44), a full update of $\texttt{OS}(\lambda)$ is obtained. As λ is a singlet spin-orbital tensor, we can simply obtain the same-spin block using Eq. (48).

Unrelaxed PDMs

The form presented in Eq. (41) is not convenient to use because of the singlet projection operator appearing in the middle of two non-singlet operators. Thus, it is natural to form separate expressions for the symmetric part and the antisymmetric part of the 2PDM tensor similarly to what is proposed in the Λ-equation solver. We define a spin-orbital tensor

$$\zeta_{a_{\sigma_1} b_{\sigma_2}}^{i_{\sigma_1} j_{\sigma_2}} = - \langle \Phi_0 | (\hat{I} + \hat{\Lambda}_2) e^{-\hat{\mathcal{Q}}} (\hat{a}_{i_{\sigma_1}}^{\dagger} \hat{a}_{j_{\sigma_2}}^{\dagger} \hat{a}_{b_{\sigma_2}} \hat{a}_{a_{\sigma_1}}) e^{\hat{\mathcal{Q}}} | \Phi_0 \rangle, \tag{63}$$

and this can be easily computed in the same way as RCCD. Using Eq. (44), $\mathtt{OS}\,(\hat{\mathcal{Q}}\xi)$ is obtained as

$$
\begin{aligned}
\mathtt{OS}\,(\hat{\mathcal{Q}}\xi) = &\frac{1}{4}\,\mathtt{symm_V}\,[\,\mathtt{symm_O}\,[\,\mathtt{OS}\,(\zeta)\,]\,] \\
&+ \frac{1}{3}\left(\frac{1}{4}\,\mathtt{asymm_V}\,[\,\mathtt{asymm_O}\,[\,\mathtt{OS}\,(\zeta)\,]+\mathtt{SS}\,(\zeta)\right).
\end{aligned} \tag{64}
$$

As $\hat{\mathcal{Q}}\xi$ is a singlet tensor, we can use Eq. (48) to form $\mathtt{SS}\,(\hat{\mathcal{Q}}\xi)$ based on $\mathtt{OS}\,(\hat{\mathcal{Q}}\xi)$ obtained above.

Applications to oligoacenes
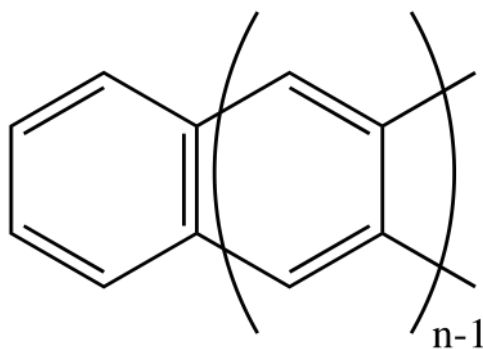
Figure 3: The chemical structure of n-acene $(C_2H_4C_{4n}H_{2n})$.

The acenes, illustrated in Fig. 3, are known to exhibit emergent strong correlations as their length grows and thus they provide a well-defined platform for testing novel approaches for strong correlations. There have been numerous studies on oligoacenes using various methods such as CASSCF,[148,149] DMRG-CASCI,[22,23] variational 2-RDM methods,[150–152] adaptive CI (ACI),[153] multi-reference averaged quadratic coupled cluster (MR-AQCC),[164,165] and density functional theory (DFT) based methods such as DFT/MRCI,[154] thermally-assisted-occupation DFT (TAO-DFT),[155] fractional-spin DFT (FS-DFT),[156] and particle-particle random-phase approximation (pp-RPA).[157] Although RCCSD has been applied to short acenes (n≤7)[149,166,167], there is no study on longer acenes using RCCSD mainly because of

their known failures for strongly correlated systems.

We compare absolute energies and natural orbital occupation numbers of different SRCC methods against the exact answers taken from ref. 22 up to 12-acene with all π-electrons correlated. The natural orbital occupation numbers for SRCC are computed with symmetrised 1PDMs. Symmetrised 1PDMs yield very similar results to unsymmetrised ones. We further study and discuss higher acenes (n>12) using CCVB-SD with a well-defined model geometry ($R_{C-C} = 1.3964\,\mathring{A}$, $R_{C-H} = 1.0755\,\mathring{A}$) not only correlating π-electrons but correlating all the valence electrons. All the calculations presented below employ a minimal basis (STO-3G) and are performed with the development version of `Q-Chem`.[161] All the plots were generated with `matplotlib`.[168]

Comparison against DMRG with all π-electrons correlated

Table 1: Reference absolute energies (in Hartrees) from the π-space DMRG calculations of ref. 22 and deviations (in mH) of several methods from the DMRG values. Geometries are also taken from ref. 22 which were optimised at the level of UB3LYP/6-31G* with $S = 0$. The number of renormalised states, M, of DMRG calculations is 1000. The DMRG calculation for n=12 was not fully converged with respect to M. Calculations with convergence problems are indicated by DNC. RHF orbitals are used for CCVB-SD, RCCSD, and RCCSD(T) whereas OD, QCCD, and QCCD(2) are computed with optimised orbitals.

n	DMRG	CCVB-SD	RCCSD	RCCSD(T)	OD	QCCD	QCCD(2)
2	-378.862173	9.472	2.509	-0.499	2.550	5.102	2.915
3	-529.721682	14.671	4.472	-0.784	4.538	8.766	5.071
4	-680.578678	20.481	6.103	-1.888	6.203	13.000	7.653
5	-831.434630	26.941	7.142	-4.185	7.254	17.846	10.706
6	-982.290070	34.822	6.432	-9.609	6.114	23.989	14.750
8	-1284.000964	54.051	DNC	DNC	DNC	DNC	DNC
10	-1585.713311	71.973	DNC	DNC	DNC	DNC	DNC
12	-1887.425575	89.154	DNC	DNC	DNC	DNC	DNC

We first examine whether using RHF orbitals is valid for these systems because the quality of RHF orbitals often degrades for strongly correlated systems. Optimised doubles (OD)[169,170] or orbital-optimised CCD yields nearly identical energies to those of RCCSD, implying that RHF orbitals are qualitatively correct. Due to convergence issues, OD was

performed only up to 6-acene, so, to further examine the efficacy of using RHF orbitals, we also carried out test CCVB-SD calculations with RBLYP orbitals. The use of RBLYP orbitals does not yield qualitatively different results. Therefore, the numbers reported in Table 1 are all obtained using stable RHF orbitals that are spatially symmetric.
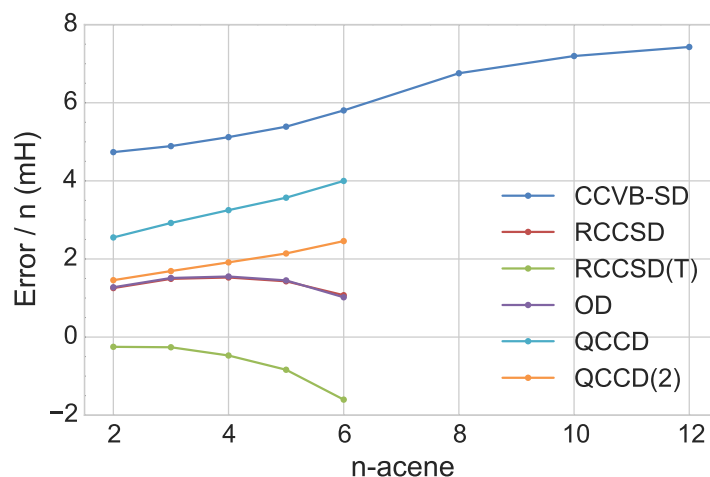

Figure 4: The correlation energy error with respect to DMRG per acene unit of different coupled-cluster methods. We note that the OD curve is right on top of the RCCSD one.

For weakly correlated systems, RCCSD and CCVB-SD yield almost identical results and the deviation between the two becomes more significant for the systems with strong correlations. For the acenes shown in Table 1, the RCCSD energies are significantly lower than those of CCVB-SD, which hints at a non-variational failure of RCCSD. More specifically, as illustrated in Table 1, RCCSD and OD may be starting to "turn over" at 6-acene because the error in correlation energies is smaller in 6-acene than in 5-acene. Moreover, the RCCSD(T) energies are lower than those of DMRG. Fig. 4 demonstrates that the correlation energy error per acene unit in CCVB-SD reaches a plateau value as the system size increases. It confirms that the correlation energy error in CCVB-SD is size-extensive. Furthermore, RCCSD, RCCSD(T), and OD turn over at 5-acene. In the end, they must plateau since they are all size-extensive.

We confirm whether RCCSD behaves non-variationally by performing orbital-optimised QCCD[100] where the left eigenfunction is improved by including a de-excitation operator up

to quadratic terms and the right eigenfunction remains the same as that of RCCD. This more balanced treatment of the left eigenfunction allows for an energy evaluation closer to that of variational CC.

Table 1 shows that the QCCD energies are above the RCCSD energies for every acene considered here. As QCCD energies are closer to the true variational CCSD energies,[88,100] we conclude that RCCSD may be behaving non-variationally even for short acenes. It is interesting that even a seemingly innocent molecule like naphthalene apparently shows non-variationality of RCCSD given that this behaviour has been mostly observed for molecules near bond dissociations. In passing, we note that CCVB-SD does not show any convergence issues unlike the others presented here and this is likely due to the approximate inclusion of connected quadruples that stabilises singles and doubles amplitudes.
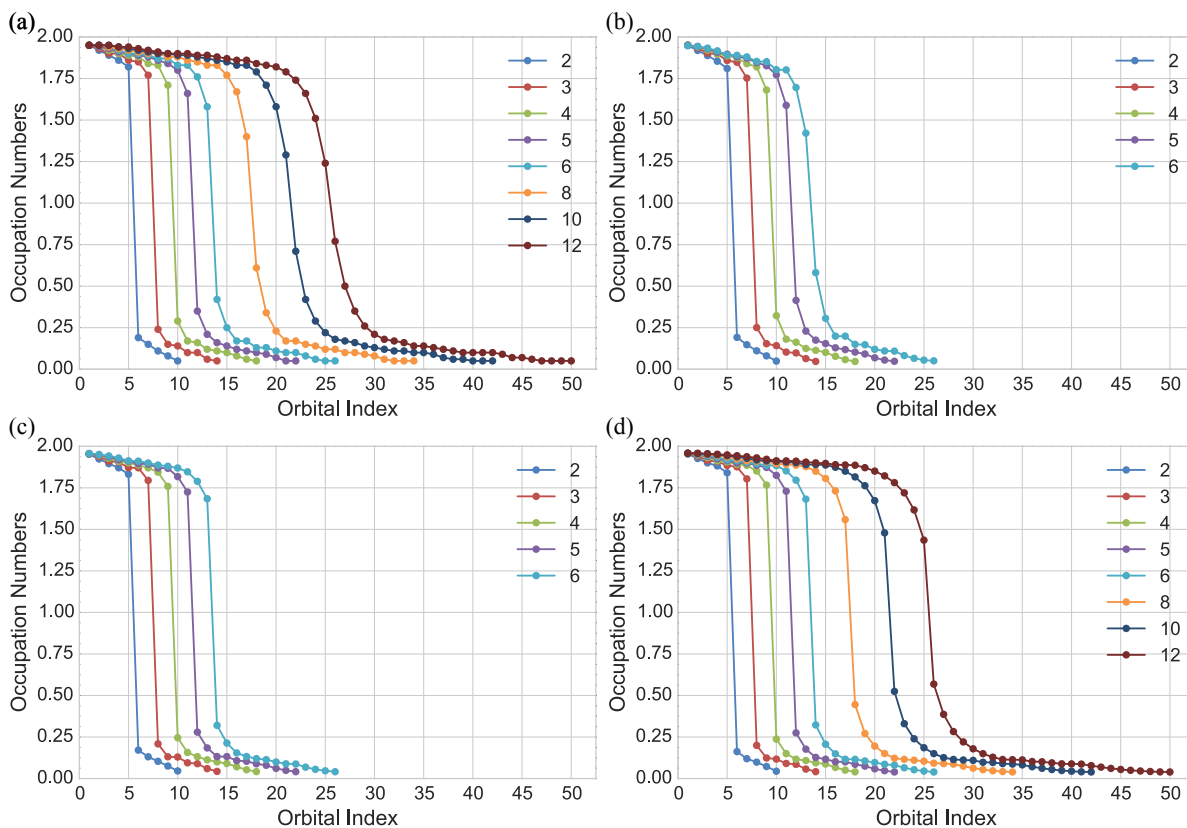
Figure 5: Natural orbital occupation numbers from (a) DMRG, (b) RCCSD, (c) QCCD, and (d) CCVB-SD.

Neither QCCD nor CCVB-SD is variational, so either could in principle exhibit non-variationality. In other words, both CCVB-SD and QCCD[88] can legitimately be below variational CCSD. QCCD cannot reach the correct limit for bond-breaking while CCVB-SD can.[100] Yet CCVB-SD yields higher energies for the acenes. This suggests that QCCD may be also exhibiting non-variationality. It will be interesting to see other approaches such as unitary CCSD[90–93] and extended CCSD[94–99] to further investigate this. In passing we note that, unlike RCCSD(T), the energies of QCCD(2),[102] which is a perturbative correction of a similar level of theory to RCCSD(T), are above the DMRG energies for acenes up to n = 6. It will be interesting to see whether QCCD(2) will become lower than DMRG for longer acenes. Given that the NOONs of QCCD and CCVB-SD are very similar and their energies are yet very different, it will be interesting to compare a perturbative correction to CCVB-SD and QCCD(2) in the future.

We then discuss the natural orbital occupation numbers (NOONs) of each method. The NOONs of RCCSD show larger polyradical character than that of DMRG, which indicates RCCSD's tendency to overcorrelate these systems. The NOONs of QCCD are less polarised than those of RCCSD and they are very similar to those of CCVB-SD. The NOONs of CCVB-SD show similar trends to DMRG's, but with smaller radical character. This may, in part, be due to missing connected higher-than-double excitations in CCVB-SD that may be necessary to better describe correlations of acenes. We discuss more in depth the nature of correlations in oligoacenes in a separate study.

Application of CCVB-SD to longer acene oligomers

We apply CCVB-SD to a model geometry up to 23-acene with all π-electrons correlated and up to 17-acene with all valence electrons correlated. As mentioned earlier, the lengths of all C-C and C-H bonds are fixed at 1.3964 Å and 1.0755 Å, respectively. The angle between three neighboring carbons and the angle between H$-$C$-$C are fixed at 120° to ensure D_{2h} symmetry.
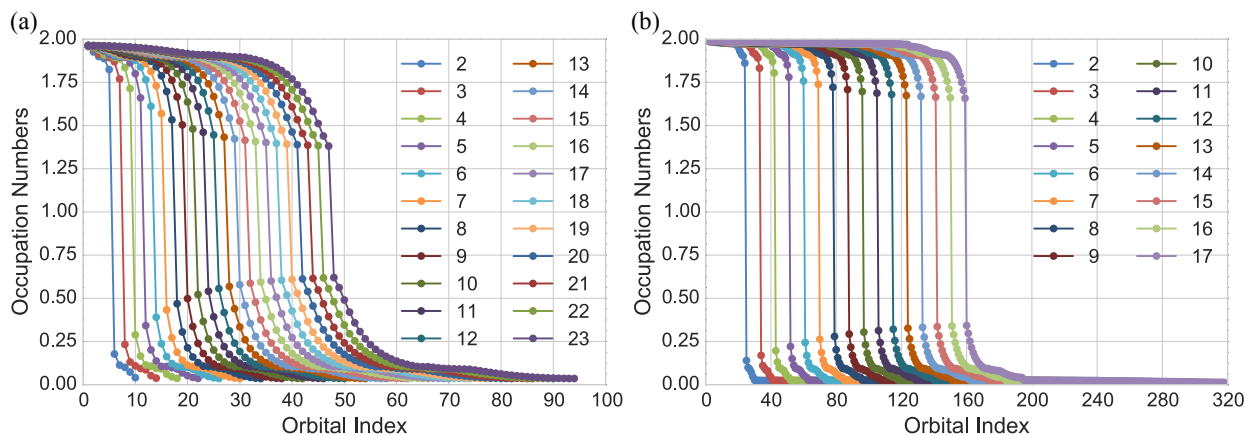
Figure 6:   Natural orbital occupation numbers of model geometries ($R_{C-C} = 1.3964$ Å, $R_{C-H} = 1.0755$ Å) from CCVB-SD with (a) all π-electrons correlated and (b) all valence electrons correlated. The largest calculation in (b) correlates 318 electrons in 318 orbitals.

The NOONs for these series are shown in Fig. 6. Compared to the results from the UB3LYP geometries used above, there is virtually no difference in the NOONs. It has been pointed out that small changes in geometries of oligoacenes do not alter their NOONs.[23] Regardless of whether all π-electrons are correlated or all valence electrons are correlated, both cases exhibit a plateau region as the acene chain length increases.

Mizukami *et al.* applied DMRG with $M = 256$ to a model geometry (R_{C-C} (shorter) = 1.402 Å, R_{C-C} (longer) = 1.435 Å, $R_{C-H} = 1.010$ Å) up to 25-acene with all π-electrons correlated, which is slightly different than the one used in this study.[23] Fitting the NOONs of HONO (highest occupied natural orbital with occupation greater than 1) and LUNO (lowest unoccupied natural orbital with occupation less than 1) to analytical functions in Fig 6 (a), the asymptotes for (HONO, LUNO) were found to be (1.36, 0.64) for CCVB-SD, whilst the ref. 23 authors obtained (1.30, 0.70) for DMRG.[171] Those $M = 256$ DMRG calculations were far from being converged with respect to the number of renormalised states and thus we expect the exact asymptotes to be closer to 1.0 for both HONO and LUNO. The π-space CCVB-SD asymptote is less radicaloid, but it qualitatively captures the emergent strong correlations present in oligoacenes.

The progression of emergent strong correlations as a function of the length of acenes

when correlating all valence electrons has not yet been well-characterised mainly because of the absence of suitable quantum chemistry models. The significant progress that has been made in developing FCIQMC[13,14] and DMRG[15–19] allows treatment of systems with approximately 100 electrons in 100 orbitals at near benchmark accuracy. However, correlating all valence electrons of the oligoacenes requires an active space much larger than this limit (e.g. even 5-acene (pentacene) has 102 electrons in 102 orbitals for the full-valence space). On the other hand, more economical wavefunction based methods such as RCCSD cannot properly describe systems with emergent strong correlations of many electrons as shown in the previous section.

Here, we apply CCVB-SD to oligoacenes up to 17-acene correlating all valence electrons, which yields a maximum active space of 318 electrons and 318 orbitals. The largest CCVB-SD calculation took little less than two hours per iteration using 32 cores in AMD Opteron Processor 6376. Under the same condition, RCCSD took roughly an hour per iteration, which confirms that the computational cost of CCVB-SD is twice larger than RCCSD.

Comparing NOONs of π-space and full-valence space calculations as illustrated in Fig. 6, it is interesting to note that the radical character in terms of NOONs is considerably less prominent for the full-valence calculations. This may be understood similarly to the way we understand two-configuration SCF (TCSCF) wavefunctions that tend to yield larger amplitudes on the excited determinants compared to the exact answers. Therefore, one would expect more radicaloid (closer to 1) NOONs for truncated active space calculations, which in our case are π-space calculations. The NOONs from the full-valence calculations also reach a plateau region as the system grows and the asymptote is (1.63, 0.37) for (HONO, LUNO).

We further compute the radical index (RI) of oligoacenes. The RI, proposed by Head-Gordon[172], is a measure of the number of radical electrons in a system. Although in terms of NOONs of HONO and LUNO the valence calculations seem to exhibit smaller radical characters than the π-space calculations, the net RI is larger in the valence calculations as
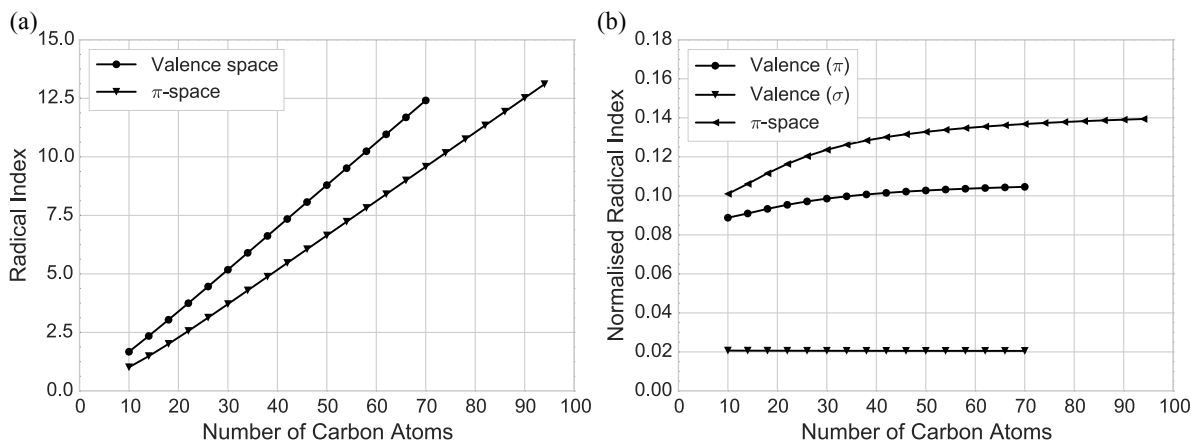
Figure 7: (a) Radical index as a function of the number of carbon atoms, and (b) normalised radical index as a function of the number of carbon atoms.

illustrated in Fig. 7 (a). This is because there are 4–5 times more correlated electrons in the valence calculations than in the π-space calculations. Therefore, we separate σ-NOs and π-NOs in the valence calculations and divide the RI by the number of σ or π-electrons, respectively. This normalised RI (NRI) directly indicates the average radical character per electron in a system and the NRI closer to 1.0 indicates more of radical character. For example, an ideal diradical would yield NRI of 1.0 within (2,2) active space. The π-NOs and σ-NOs are classfied by their irreducible representations as the NOs from CCVB-SD are all spatially symmetric in the systems considered in this work.

With this classification, the resulting NRI is depicted in Fig. 7 (b). Unsurprisingly, the σ-NOs in the valence calculations do not show any noticeable changes in the NRI and their NRIs are much smaller than those of π-NOs. The NRI of valence-π is smaller than that of π-space calculations, which is consistent with what is observed in the NOONs. The NRIs of π-NOs increase as system grows and they reach bulk values in both valence and π-space calculations. This clearly shows the progressive emergent radical character in the π-space of oligoacenes. In passing, we note that increasing the basis beyond STO-3G is expected to show a further reduction in the largest NOONs for virtuals and this is an interesting subject of future study.

Conclusions and Outlook

In this paper, we summarized the CCVB-SD electron correlation method in terms of orthogonally spin-adapted doubles operators and derived its Λ-equation and unrelaxed density matrices. We also described a block-tensor based implementation of CCVB-SD and showed a large-scale application to acene oligomers correlating up to 318 electrons in 318 orbitals.

Studying oligoacenes with CCVB-SD and other single reference CC methods, several interesting results were found: (1) Even for naphthalene, a significant difference in energy between RCCSD and QCCD was found, which suggests non-variational behaviour of RCCSD. This non-variational behaviour becomes more pronounced for larger acenes. (2) CCVB-SD qualitatively captures strong correlations of acenes based on the comparison between NOONs from CCVB-SD and DMRG [22,23] and (3) correlating all valence electrons shows a significantly smaller radical character in the π-space than when correlating only the π-electrons, but it still shows progressive emergent strong correlations as system grows.

Lack of connected excitation beyond double in CCVB-SD is possibly the largest missing contribution, with triples (T) being the leading correction. In the future, modifications of CCVB-SD to include T (and beyond) are desirable. There are many ways to pursue this direction including non-iterative approaches as is done in similarity-transformed perturbation theory,[173] CCSD(T),[76] and optimised-inner-projection method that has been applied to incorporate T into ACPQ.[174–176] Approximating T in a self-contained iterative fashion using singles and doubles similarly to the way CCVB-SD approximates connected quadruples (Q) would be formally and computationally more satisfying but is still an open question.

There are other future extensions of CCVB-SD to consider such as linear-response CC (LR-CC)[177] or equation-of-motion CC (EOM-CC)[178] for excited states and open-shell CCVB-SD similar to open-shell CCVB.[179] As CCVB-SD handles valence correlations well, for basis sets larger than minimal basis, it would be beneficial to develop valence optimised CCVB-D similarly to valence optimised doubles (VOD).[180] It will be interesting to study mechanisms of reactions involving strongly correlated transition states such as pericyclic reactions us-

ing algorithms such as nudged elastic band[181,182] and growing string methods.[183–186] The production-level implementation of CCVB-SD energy and gradients described in this paper will facilitate these exciting developments and applications.

Acknowledgements

Appendix

Proof of Eq. (25)

We begin with Eq. (63) and Eq. (64) of ref. 143 in our present notation,

$$\hat{\mathcal{S}} = \frac{1}{2} \sum_{ijab} S_{ij}^{ab} \, \hat{\Sigma}_{ij}^{ab}, \tag{A1}$$

$$\hat{\mathcal{Q}} = \frac{1}{2} \sum_{ijab} S_{ij}^{ab} \, {}^{tt}\hat{\kappa}_{ij}^{ab} \tag{A2}$$

$$= \sum_{\substack{i<j \\ a<b}} \left(S_{ij}^{ab} - S_{ji}^{ab} \right) {}^{tt}\hat{\kappa}_{ij}^{ab}, \tag{A3}$$

where t_{ij}^{ab}, $\mathcal{S}_{ij}^{ab}$, and $\mathcal{Q}_{ij}^{ab}$ in ref. 143 correspond to S_{ij}^{ab}, $\hat{\Sigma}_{ij}^{ab}$, and ${}^{tt}\hat{\kappa}_{ij}^{ab}$, respectively.

Therefore, we write

$$Q_{ij}^{ab} = S_{ij}^{ab} - S_{ji}^{ab}. \tag{A4}$$

In terms of ${}^{ss}\hat{\Sigma}_{ij}^{ab}$ and ${}^{tt}\hat{\Sigma}_{ij}^{ab}$, $\hat{\Sigma}_{ij}^{ab}$ is written as

$$\hat{\Sigma}_{ij}^{ab} = -\frac{\sqrt{3}}{2} \, {}^{ss}\hat{\Sigma}_{ij}^{ab} - \frac{1}{2} \, {}^{tt}\hat{\Sigma}_{ij}^{ab}. \tag{A5}$$

For any $i \neq j$ and $a \neq b$, using Eq. (A5) one can show that the terms in Eq. (17) and Eq. (A1) pertinent to these indices are

$$S_{ij}^{ab} \, \hat{\Sigma}_{ij}^{ab} + S_{ji}^{ab} \, \hat{\Sigma}_{ji}^{ab} = -\frac{\sqrt{3}}{2} \left(S_{ij}^{ab} + S_{ji}^{ab} \right) {}^{ss}\hat{\Sigma}_{ij}^{ab} - \frac{1}{2} \left(S_{ij}^{ab} - S_{ji}^{ab} \right) {}^{tt}\hat{\Sigma}_{ij}^{ab} \tag{A6}$$

$$= {}^{S}S_{ij}^{ab} \, {}^{ss}\hat{\Sigma}_{ij}^{ab} + {}^{A}S_{ij}^{ab} \, {}^{tt}\hat{\Sigma}_{ij}^{ab}, \tag{A7}$$

which gives

$$ {}^{S}S_{ij}^{ab} = -\frac{\sqrt{3}}{2} \left(S_{ij}^{ab} + S_{ji}^{ab} \right), \tag{A8}$$

$$ {}^{A}S_{ij}^{ab} = -\frac{1}{2} \left(S_{ij}^{ab} - S_{ji}^{ab} \right). \tag{A9}$$

Comparing Eq. (A9) and Eq. (A4) proves Eq. (25).

Table of Contents Figure
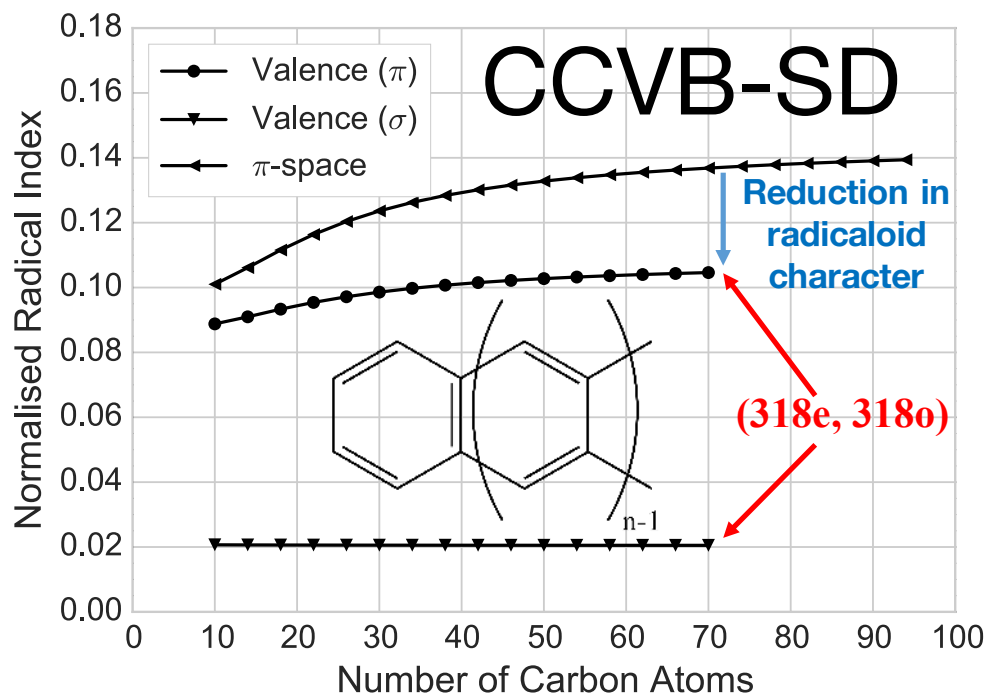
References

(1) Blomberg, M. R. A.; Borowski, T.; Himo, F.; Liao, R.-Z.; Siegbahn, P. E. M. *Chem. Rev.* **2014**, *114*, 3601–3658.

(2) McEvoy, J. P.; Brudvig, G. W. *Chem. Rev.* **2006**, *106*, 4455–4483.

(3) Mukhopadhyay, S.; Mandal, S. K.; Bhaduri, S.; Armstrong, W. H. *Chem. Rev.* **2004**, *104*, 3981–4026.

(4) Savéant, J.-M. *Adv. Phys. Org. Chem.* **2000**, *35*, 117–192.

(5) Huang, R.; Phan, H.; Herng, T. S.; Hu, P.; Zeng, W.; Dong, S.-q.; Das, S.; Shen, Y.; Ding, J.; Casanova, D.; Wu, J. *J. Am. Chem. Soc* **2016**, *138*, 10323–10330.

(6) Hinkel, F.; Freudenberg, J.; Bunz, U. H. F. *Angew. Chem. Int. Ed. Engl.* **2016**,

(7) Trinquier, G.; Malrieu, J.-P. *Chem. Eur. J* **2015**, *21*, 814–828.

(8) Hu, P.; Lee, S.; Herng, T. S.; Aratani, N.; Gonçalves, T. P.; Qi, Q.; Shi, X.; Yamada, H.; Huang, K.-W.; Ding, J.; Kim, D.; Wu, J. *J. Am. Chem. Soc* **2015**,

(9) Sadowsky, D.; McNeill, K.; Cramer, C. J. *Farad. Discuss.* **2010**, *145*, 507–521.

(10) Dai, P. *Rev. Mod. Phys.* **2015**, *87*, 855–896.

(11) Georges, A.; Kotliar, G.; Krauth, W.; Rozenberg, M. J. *Rev. Mod. Phys.* **1996**, *68*, 13–125.

(12) Szalay, P. G.; Müller, T.; Gidofalvi, G.; Lischka, H.; Shepard, R. *Chem. Rev.* **2012**, *112*, 108–181.

(13) Booth, G. H.; Thom, A. J. W.; Alavi, A. *J. Chem. Phys.* **2009**, *131*, 054106.

(14) Cleland, D.; Booth, G. H.; Alavi, A. *J. Chem. Phys.* **2010**, *132*, 041103.

(15) White, S. R. *Phys. Rev. Lett.* **1992**, *69*, 2863–2866.

(16) White, S. R. *Phys. Rev. B* **1993**, *48*, 10345–10356.

(17) White, S. R.; Martin, R. L. *J. Chem. Phys.* **1999**, *110*, 4127.

(18) Schollwöck, U. *Ann. Phys.* **2011**, *326*, 96–192.

(19) Schollwöck, U. *Phil. Trans. R. Soc. A.* **2011**, *369*, 2643–61.

(20) Knowles, P.; Handy, N. *Chem. Phys. Lett.* **1984**, *111*, 315–321.

(21) Knowles, P. J.; Handy, N. C. *Comput. Phys. Commun.* **1989**, *54*, 75–83.

(22) Hachmann, J.; Dorando, J. J.; Avils, M.; Chan, G. K.-L. *J. Chem. Phys.* **2007**, *127*, 134309.

(23) Mizukami, W.; Kurashige, Y.; Yanai, T. *J. Chem. Theory Comput.* **2013**, *9*, 401–407.

(24) Kurashige, Y.; Chan, G. K.-L.; Yanai, T. *Nat. Chem.* **2013**, *5*, 660–6.

(25) Sharma, S.; Sivalingam, K.; Neese, F.; Chan, G. K.-L. *Nat. Chem.* **2014**, *6*, 927–33.

(26) Daday, C.; Smart, S.; Booth, G. H.; Alavi, A.; Filippi, C. *J. Chem. Theory Comput.* **2012**, *8*, 4441–4451.

(27) Cleland, D.; Booth, G. H.; Overy, C.; Alavi, A. *J. Chem. Theory Comput.* **2012**, *8*, 4138–4152.

(28) Booth, G. H.; Grüneis, A.; Kresse, G.; Alavi, A. *Nature* **2013**, *493*, 365–70.

(29) Thomas, R. E.; Booth, G. H.; Alavi, A. *Phys. Rev. Lett.* **2015**, *114*, 033001.

(30) Bartlett, R. J.; Musiał, M. *Rev. Mod. Phys.* **2007**, *79*, 291–352.

(31) Lyakh, D. I.; Musiał, M.; Lotrich, V. F.; Bartlett, R. J. *Chem. Rev.* **2012**, *112*, 182–243.

(32) Köhn, A.; Hanauer, M.; Mück, L. A.; Jagau, T.-C.; Gauss, J. *Wiley Interdiscip. Rev. Comput. Mol. Sci.* **2013**, *3*, 176–197.

(33) Jeziorski, B.; Monkhorst, H. J. *Phys. Rev. A* **1981**, *24*, 1668–1681.

(34) Balková, A.; Kucharski, S. A.; Meissner, L.; Bartlett, R. J. *Theor. Chim. Acta* **1991**, *80*, 335–348.

(35) Kucharski, S. A.; Balkov, A.; Szalay, P. G.; Bartlett, R. J. *J. Chem. Phys.* **1992**, *97*, 4289.

(36) Piecuch, P.; Paldus, J. *Theor. Chim. Acta* **1992**, *83*, 69–103.

(37) Evangelista, F. A.; Allen, W. D.; Schaefer, H. F. *J. Chem. Phys.* **2006**, *125*, 154113.

(38) Datta, D.; Mukherjee, D. *J. Chem. Phys.* **2009**, *131*, 044124.

(39) Lindgren, I.; Mukherjee, D. *Phys. Rep.* **1987**, *151*, 93–127.

(40) Lindgren, I. *Phys. Scripta* **1985**, *32*, 291–302.

(41) Mukherjee, D.; Moitra, R. K.; Mukhopadhyay, A. *Mol. Phys.* **1977**, *33*, 955–969.

(42) Stolarczyk, L. Z.; Monkhorst, H. J. *Int. J. Quantum Chem.* **1984**, *26*, 267–291.

(43) Stolarczyk, L. Z.; Monkhorst, H. J. *Phys. Rev. A* **1985**, *32*, 725–742.

(44) Stolarczyk, L. Z.; Monkhorst, H. J. *Phys. Rev. A* **1985**, *32*, 743–747.

(45) Stolarczyk, L. Z.; Monkhorst, H. J. *Phys. Rev. A* **1988**, *37*, 1908–1925.

(46) Stolarczyk, L. Z.; Monkhorst, H. J. *Phys. Rev. A* **1988**, *37*, 1926–1933.

(47) Stolarczyk, L. Z.; Monkhorst, H. J. *Mol. Phys.* **2010**, *108*, 3067–3089.

(48) Fang, T.; Shen, J.; Li, S. *J. Chem. Phys.* **2008**, *128*, 224107.

(49) Datta, D.; Kong, L.; Nooijen, M. *J. Chem. Phys.* **2011**, *134*, 214116.

(50) Fang, T.; Li, S. *J. Chem. Phys.* **2007**, *127*, 204108.

(51) Hanauer, M.; Köhn, A. *J. Chem. Phys.* **2011**, *134*, 204111.

(52) Evangelista, F. A.; Gauss, J. *J. Chem. Phys.* **2011**, *134*, 114102.

(53) Kinoshita, T.; Hino, O.; Bartlett, R. J. *J. Chem. Phys.* **2005**, *123*, 074106.

(54) Lyakh, D. I.; Ivanov, V. V.; Adamowicz, L. *J. Chem. Phys.* **2005**, *122*, 024108.

(55) Hanrath, M. *J. Chem. Phys.* **2005**, *123*, 084102.

(56) Pittner, J.; Šmydke, J.; Čársky, P.; Hubač, I. *J. Mol. Struc.-THEOCHEM* **2001**, *547*, 239–244.

(57) Hubač, I.; Wilson, S. *J. Phys. B: At., Mol. Opt. Phys.* **2000**, *33*, 365–374.

(58) Hubač, I.; Pittner, J.; Čársky, P. *J. Chem. Phys.* **2000**, *112*, 8779.

(59) Pittner, J.; Nachtigall, P.; Čársky, P.; Hubač, I. *J. Phys. Chem. A* **2001**, *105*, 1354–1356.

(60) Chattopadhyay, S.; Mahapatra, U. S.; Mukherjee, D. *J. Chem. Phys.* **2000**, *112*, 7939.

(61) Kong, L. *Int. J. Quantum Chem.* **2009**, *109*, 441–447.

(62) Chattopadhyay, S.; Mahapatra, U. S.; Mukherjee, D. *J. Chem. Phys.* **1999**, *111*, 3820.

(63) Pittner, J. *J. Chem. Phys.* **2003**, *118*, 10876.

(64) Mahapatra, U. S.; Datta, B.; Mukherjee, D. *J. Chem. Phys.* **1999**, *110*, 6171.

(65) Mahapatra, U. S.; Datta, B.; Mukherjee, D. *Mol. Phys.* **2010**,

(66) Mášik, J.; Hubač, I.; Mach, P. *J. Chem. Phys.* **1998**, *108*, 6571.

(67) Mášik, J.; Hubač, I. *Collect. Czech. Chem. Commun.* **1997**, *62*, 829–842.

(68) Hubač, I.; Neogrády, P. *Phys. Rev. A* **1994**, *50*, 4558–4564.

(69) Adamowicz, L.; Malrieu, J.-P.; Ivanov, V. V. *J. Chem. Phys.* **2000**, *112*, 10075.

(70) Kállay, M.; Szalay, P. G.; Surján, P. R. *J. Chem. Phys.* **2002**, *117*, 980.

(71) Piecuch, P.; Kowalski, K. *Int. J. Mol. Sci.* **2002**, *3*, 676–709.

(72) Schucan, T.; Weidenmüller, H. *Ann. Phys.* **1972**, *73*, 108–135.

(73) Kaldor, U. *Phys. Rev. A* **1988**, *38*, 6013–6016.

(74) Malrieu, J. P.; Durand, P.; Daudey, J. P. *J. Phys. A: Math. Gen.* **1985**, *18*, 809–826.

(75) Jankowski, K.; Malinowski, P. *J. Phys. B: At., Mol. Opt. Phys.* **1994**, *27*, 1287–1298.

(76) Raghavachari, K.; Trucks, G. W.; Pople, J. A.; Head-Gordon, M. *Chem. Phys. Lett.* **1989**, *157*, 479–483.

(77) Taube, A. G.; Bartlett, R. J. *J. Chem. Phys.* **2008**, *128*, 044110.

(78) Włoch, M.; Gour, J. R.; Piecuch, P. *J. Phys. Chem. A* **2007**, *111*, 11359–11382.

(79) Kowalski, K.; Piecuch, P. *Chem. Phys. Lett.* **2001**, *344*, 165–175.

(80) Piecuch, P.; Kowalski, K.; Pimienta, I. S. O.; Fan, P.-D.; Lodriguito, M.; McGuire, M. J.; Kucharski, S. A.; Kuś, T.; Musiał, M. *Theor. Chem. Acc.* **2004**, *112*, 349–393.

(81) Kowalski, K.; Piecuch, P. *J. Chem. Phys.* **2000**, *113*, 5644.

(82) Piecuch, P.; Kowalski, K.; Pimienta, I. S. O.; Mcguire, M. J. *Int. Rev. Phys. Chem.* **2002**, *21*, 527–655.

(83) Piecuch, P.; Włoch, M. *J. Chem. Phys.* **2005**, *123*, 224105.

(84) Kowalski, K.; Piecuch, P. *J. Chem. Phys.* **2000**, *113*, 18.

(85) Piecuch, P.; Kucharski, S. A.; Kowalski, K.; Musiał, M. *Comput. Phys. Commun.* **2002**, *149*, 71–96.

(86) Kowalski, K.; Piecuch, P. *J. Chem. Phys.* **2004**, *120*, 1715.

(87) Van Voorhis, T.; Head-Gordon, M. *J. Chem. Phys.* **2000**, *113*, 8873.

(88) Cooper, B.; Knowles, P. J. *J. Chem. Phys.* **2010**, *133*, 234102.

(89) Bartlett, R. J.; Noga, J. *Chem. Phys. Lett.* **1988**, *150*, 29–36.

(90) Hoffmann, M. R.; Simons, J. *J. Chem. Phys.* **1988**, *88*, 993.

(91) Pal, S. *Theor. Chim. Acta* **1984**, *66*, 207–215.

(92) Bartlett, R. J.; Kucharski, S. A.; Noga, J. *Chem. Phys. Lett.* **1989**, *155*, 133–140.

(93) Watts, J. D.; Trucks, G. W.; Bartlett, R. J. *Chem. Phys. Lett.* **1989**, *157*, 359–366.

(94) Pal, S. *Phys. Rev. A* **1986**, *34*, 2682–2686.

(95) Basu Kumar, A.; Vaval, N.; Pal, S. *Chem. Phys. Lett.* **1998**, *295*, 189–194.

(96) Manohar, P. U.; Vaval, N.; Pal, S. *Chem. Phys. Lett.* **2004**, *387*, 442–447.

(97) Fan, P.-D.; Kowalski, K.; Piecuch, P. *Mol. Phys.* **2005**, *103*, 2191–2213.

(98) Fan, P.-D.; Piecuch, P. *Adv. Quantum Chem.* **2006**, *51*, 1–57.

(99) Arponen, J. *Ann. Phys.* **1983**, *151*, 311–382.

(100) Van Voorhis, T.; Head-Gordon, M. *Chem. Phys. Lett.* **2000**, *330*, 585–594.

(101) Byrd, E. F. C.; Van Voorhis, T.; Head-Gordon, M. *J. Phys. Chem. B* **2002**, *106*, 8070–8077.

(102) Gwaltney, S. R.; Byrd, E. F.; Van Voorhis, T.; Head-Gordon, M. *Chem. Phys. Lett.* **2002**, *353*, 359–367.

(103) Noga, J.; Bartlett, R. J. *J. Chem. Phys.* **1987**, *86*, 7041.

(104) Oliphant, N.; Adamowicz, L. *J. Chem. Phys.* **1991**, *95*, 6645.

(105) Parkhill, J. A.; Lawler, K.; Head-Gordon, M. *J. Chem. Phys.* **2009**, *130*, 084101.

(106) Parkhill, J. A.; Head-Gordon, M. *J. Chem. Phys.* **2010**, *133*, 024103.

(107) Parkhill, J. A.; Azar, J.; Head-Gordon, M. *J. Chem. Phys.* **2011**, *134*, 154112.

(108) Lehtola, S.; Parkhill, J.; Head-Gordon, M. *J. Chem. Phys.* **2016**, *145*, 134110.

(109) Krylov, A. I. *Chem. Phys. Lett.* **2001**, *338*, 375–384.

(110) Slipchenko, L. V.; Krylov, A. I. *J. Chem. Phys.* **2002**, *117*, 4694.

(111) Krylov, A. I. *Acc. Chem. Res.* **2006**, *39*, 83–91.

(112) Krylov, A. I. *Ann. Rev. Phys. Chem.* **2008**, *59*, 433–462.

(113) Paldus, J.; Čížek, J.; Takahashi, M. *Phys. Rev. A* **1984**, *30*, 2193–2209.

(114) Paldus, J.; Takahashi, M.; Cho, R. W. H. *Phys. Rev. B* **1984**, *30*, 4267–4291.

(115) Jankowski, K.; Paldus, J. *Int. J. Quantum Chem.* **1980**, *18*, 1243–1269.

(116) Adams, B. G.; Jankowski, K.; Paldus, J. *Phys. Rev. A* **1981**, *24*, 2330–2338.

(117) Chiles, R. A.; Dykstra, C. E. *Chem. Phys. Lett.* **1981**, *80*, 69–72.

(118) Dykstra, C. E.; Liu, S.-y.; Daskalakis, M. F.; Lucia, J. P.; Takahashi, M. *Chem. Phys. Lett.* **1987**, *137*, 266–272.

(119) Taube, A. G.; Bartlett, R. J. *J. Chem. Phys.* **2009**, *130*, 144112.

(120) Bartlett, R. J.; Musiał, M. *J. Chem. Phys.* 204105.

(121) Meyer, W. *Theor. Chim. Acta* **1974**, *35*, 277–292.

(122) Ahlrichs, R.; Lischka, H.; Staemmler, V.; Kutzelnigg, W. *J. Chem. Phys.* **1975**, *62*, 1225.

(123) Kats, D.; Manby, F. R. *J. Chem. Phys.* **2013**, *139*, 021102.

(124) Kats, D. *J. Chem. Phys.* **2016**, *144*, 044102.

(125) Kats, D. *J. Chem. Phys.* **2014**, *141*, 061101.

(126) Rishi, V.; Perera, A.; Bartlett, R. J. *J. Chem. Phys.* **2016**, *144*, 124117.

(127) Bulik, I. W.; Henderson, T. M.; Scuseria, G. E. *J. Chem. Theory Comput.* **2015**, *11*, 3171–3179.

(128) Paldus, J. *J. Chem. Phys.* **1977**, *67*, 303.

(129) Adams, B. G.; Paldus, J. *Phys. Rev. A* **1979**, *20*, 1–17.

(130) Geertsen, J.; Oddershede, J. *J. Chem. Phys.* **1986**, *85*, 2112.

(131) Piecuch, P.; Paldus, J. *Int. J. Quantum Chem.* **1989**, *36*, 429–453.

(132) This is confirmed with our in–house code. Once CCVB–SD is implemented, CCSD0 can be easily implemented by removing antisymmetric doubles terms in the CCVB–SD equation.

(133) Gomez, J. A.; Henderson, T. M.; Scuseria, G. E. *J. Chem. Phys.* **2016**, *145*, 134103.

(134) Paldus, J.; Li, X. *Collect. Czech. Chem. Commun.* **2003**, *68*, 554–586.

(135) Stolarczyk, L. Z. *Chem. Phys. Lett.* **1994**, *217*, 1–6.

(136) Li, X.; Peris, G.; Planelles, J.; Rajadall, F.; Paldus, J. *J. Chem. Phys.* **1997**, *107*, 90.

(137) Paldus, J.; Planelles, J. *Theor. Chim. Acta* **1994**, *89*, 13–31.

(138) Planelles, J.; Paldus, J.; Li, X. *Theor. Chim. Acta* **1994**, *89*, 33–57.

(139) Planelles, J.; Paldus, J.; Li, X. *Theor. Chim. Acta* **1994**, *89*, 59–76.

(140) Piecuch, P.; Toboła, R.; Paldus, J. *Int. J. Quantum Chem.* **1995**, *55*, 133–146.

(141) Piecuch, P.; Toboła, R.; Paldus, J. *Phys. Rev. A* **1996**, *54*, 1210–1241.

(142) Löwdin, P.-O. *Phys. Lett.* **1955**, *97*, 1509–1520.

(143) Small, D. W.; Head-Gordon, M. *J. Chem. Phys.* **2012**, *137*, 114103.

(144) Small, D. W.; Head-Gordon, M. *J. Chem. Phys.* **2009**, *130*, 084103.

(145) Small, D. W.; Head-Gordon, M. *Phys. Chem. Chem. Phys.* **2011**, *13*, 19285–97.

(146) Small, D. W.; Lawler, K. V.; Head-Gordon, M. *J. Chem. Theory Comput.* **2014**, *10*, 2027–40.

(147) Qiu, Y.; Henderson, T. M.; Scuseria, G. E. *J. Chem. Phys.* **2016**, *145*, 111102.

(148) Bendikov, M.; Duong, H. M.; Starkey, K.; Houk, K. N.; Carter, E. A.; Wudl, F. *J. Am. Chem. Soc* **2004**, *126*, 7416–7417.

(149) Hajgat, B.; Szieberth, D.; Geerlings, P.; De Proft, F.; Deleuze, M. S. *J. Chem. Phys.* **2009**, *131*, 224321.

(150) Pelzer, K.; Greenman, L.; Gidofalvi, G.; Mazziotti, D. A. *J. Phys. Chem. A* **2011**, *115*, 5632–5640.

(151) Fosso-Tande, J.; Nascimento, D. R.; DePrince, A. E. *Mol. Phys.* **2015**, 1–8.

(152) Fosso-Tande, J.; Nguyen, T.-S.; Gidofalvi, G.; DePrince, A. E. *J. Chem. Theory Comput.* **2016**, *12*, 2260–2271.

(153) Schriber, J. B.; Evangelista, F. A. *J. Chem. Phys.* **2016**, *144*, 161106.

(154) Bettinger, H. F.; Tönshoff, C.; Doerr, M.; Sanchez-Garcia, E. *J. Chem. Theory Comput.* **2016**, *12*, 305–312.

(155) Chai, J.-D. *J. Chem. Phys.* **2012**, *136*, 154104.

(156) Ess, D. H.; Johnson, E. R.; Hu, X.; Yang, W. *J. Phys. Chem. A* **2011**, *115*, 76–83.

(157) Yang, Y.; Davidson, E. R.; Yang, W. *Proc. Natl. Acad. Sci. U.S.A.* **2016**, *113*, E5098–E5107.

(158) Gerratt, J.; Cooper, D. L.; Karadakov, P. B.; Raimondi, M. *Chem. Soc. Rev.* **1997**, *26*, 87.

(159) Goddard, W. A.; Harding, L. B. *Ann. Rev. Phys. Chem.* **1978**, *29*, 363–396.

(160) Shavitt, I.; Bartlett, R. J. *Many-Body Methods in Chemistry and Physics: MBPT and Coupled-Cluster Theory*; Cambridge University Press, 2009; pp 347–405.

(161) Shao, Y.; Gan, Z.; Epifanovsky, E.; Gilbert, A. T.; Wormit, M.; Kussmann, J.; Lange, A. W.; Behn, A.; Deng, J.; Feng, X.; Ghosh, D.; Goldey, M.; Horn, P. R.; Jacobson, L. D.; Kaliman, I.; Khaliullin, R. Z.; Kuś, T.; Landau, A.; Liu, J.; Proynov, E. I.; Rhee, Y. M.; Richard, R. M.; Rohrdanz, M. A.; Steele, R. P.; Sundstrom, E. J.; Woodcock, H. L.; Zimmerman, P. M.; Zuev, D.; Albrecht, B.; Alguire, E.; Austin, B.; Beran, G. J. O.; Bernard, Y. A.; Berquist, E.; Brandhorst, K.; Bravaya, K. B.; Brown, S. T.; Casanova, D.; Chang, C.-M.; Chen, Y.; Chien, S. H.; Closser, K. D.; Crittenden, D. L.; Diedenhofen, M.; DiStasio, R. A.; Do, H.; Dutoi, A. D.; Edgar, R. G.; Fatehi, S.; Fusti-Molnar, L.; Ghysels, A.; Golubeva-Zadorozhnaya, A.; Gomes, J.; Hanson-Heine, M. W.; Harbach, P. H.; Hauser, A. W.; Hohenstein, E. G.; Holden, Z. C.; Jagau, T.-C.; Ji, H.; Kaduk, B.; Khistyaev, K.; Kim, J.; Kim, J.; King, R. A.; Klunzinger, P.; Kosenkov, D.; Kowalczyk, T.; Krauter, C. M.; Lao, K. U.; Laurent, A. D.; Lawler, K. V.; Levchenko, S. V.; Lin, C. Y.; Liu, F.; Livshits, E.; Lochan, R. C.; Luenser, A.; Manohar, P.; Manzer, S. F.; Mao, S.-P.; Mardirossian, N.; Marenich, A. V.; Maurer, S. A.; Mayhall, N. J.; Neuscamman, E.; Oana, C. M.; Olivares-Amaya, R.; O'Neill, D. P.; Parkhill, J. A.; Perrine, T. M.; Peverati, R.; Prociuk, A.; Rehn, D. R.; Rosta, E.; Russ, N. J.; Sharada, S. M.; Sharma, S.; Small, D. W.; Sodt, A.; Stein, T.; Stück, D.; Su, Y.-C.; Thom, A. J.; Tsuchimochi, T.; Vanovschi, V.; Vogt, L.; Vydrov, O.; Wang, T.; Watson, M. A.; Wenzel, J.; White, A.; Williams, C. F.; Yang, J.; Yeganeh, S.; Yost, S. R.; You, Z.-Q.; Zhang, I. Y.; Zhang, X.; Zhao, Y.; Brooks, B. R.; Chan, G. K.; Chipman, D. M.; Cramer, C. J.; Goddard, W. A.; Gordon, M. S.; Hehre, W. J.; Klamt, A.; Schaefer, H. F.; Schmidt, M. W.; Sherrill, C. D.; Truhlar, D. G.; Warshel, A.; Xu, X.; Aspuru-Guzik, A.; Baer, R.; Bell, A. T.; Besley, N. A.; Chai, J.-D.; Dreuw, A.; Dunietz, B. D.; Furlani, T. R.; Gwaltney, S. R.; Hsu, C.-P.; Jung, Y.; Kong, J.; Lam-

brecht, D. S.; Liang, W.; Ochsenfeld, C.; Rassolov, V. A.; Slipchenko, L. V.; Subotnik, J. E.; Van Voorhis, T.; Herbert, J. M.; Krylov, A. I.; Gill, P. M.; Head-Gordon, M. *Mol. Phys.* **2015**, *113*, 184–215.

(162) Epifanovsky, E.; Wormit, M.; Kuś, T.; Landau, A.; Zuev, D.; Khistyaev, K.; Manohar, P.; Kaliman, I.; Dreuw, A.; Krylov, A. I. *J. Comput. Chem* **2013**, *34*, 2293–2309.

(163) Pulay, P. *Chem. Phys. Lett.* **1980**, *73*, 393 – 398.

(164) Plasser, F.; Pašalić, H.; Gerzabek, M. H.; Libisch, F.; Reiter, R.; Burgdörfer, J.; Müller, T.; Shepard, R.; Lischka, H. *Angew. Chem. Int. Ed. Engl.* **2013**, *52*, 2581–2584.

(165) Horn, S.; Plasser, F.; Müller, T.; Libisch, F.; Burgdörfer, J.; Lischka, H. *Theor. Chem. Acc.* **2014**, *133*, 1511.

(166) Deleuze, M. S.; Claes, L.; Kryachko, E. S.; Franois, J.-P. *J. Chem. Phys.* **2003**, *119*, 3106.

(167) Rangel, T.; Hamed, S. M.; Bruneval, F.; Neaton, J. B. *J. Chem. Theory Comput.* **2016**, *12*, 2834–2842.

(168) Hunter, J. D. *Comput. Sci. Eng.* **2007**, *9*, 90–95.

(169) Sherrill, C. D.; Krylov, A. I.; Byrd, E. F. C.; Head-Gordon, M. *J. Chem. Phys.* **1998**, *109*, 4171.

(170) Bozkaya, U.; Turney, J. M.; Yamaguchi, Y.; Schaefer, H. F.; Sherrill, C. D. *J. Chem. Phys.* **2011**, *135*, 104103.

(171) We used an exponential fit $[a + b\exp[cn]]$ for CCVB–SD whereas the DMRG study in ref. 23 employed a different fit $[2 - a(1 + \tanh[c(n - b)])]$ for HONO and LUNO is

constructed by $2 - n_{\text{HONO}}$. Moreover, when fitting CCVB–SD data we took only points with n > 5. We prefer using the exponential fit because it yields asymptotes closer to 1 than the longest acene's HONO and LUNO occupation numbers whilst the hyperbolic tangent fit does not.

(172) Head-Gordon, M. *Chem. Phys. Lett.* **2003**, *372*, 508–511.

(173) Gwaltney, S. R.; Head-Gordon, M. *Chem. Phys. Lett.* **2000**, *323*, 21–28.

(174) Piecuch, P.; Zarrabian, S.; Paldus, J.; Čížek, J. *Phys. Rev. A* **1990**, *42*, 5155–5167.

(175) Piecuch, P.; Zarrabian, S.; Paldus, J.; Čížek, J. *Phys. Rev. B* **1990**, *42*, 3351–3379.

(176) Piecuch, P.; Paldus, J. *Theor. Chim. Acta* **1990**, *78*, 65–128.

(177) Sekino, H.; Bartlett, R. J. *Int. J. Quantum Chem.* **1984**, *26*, 255–265.

(178) Gwaltney, S. R.; Nooijen, M.; Bartlett, R. J. *Chem. Phys. Lett.* **1996**, *248*, 189–198.

(179) Manuscript is in preparation by two of us (D.W.S. and M.H.–G.).

(180) Krylov, A. I.; Sherrill, C. D.; Byrd, E. F. C.; Head-Gordon, M. *J. Chem. Phys.* **1998**, *109*, 10669.

(181) Henkelman, G.; Uberuaga, B. P.; Jónsson, H. *J. Chem. Phys.* **2000**, *113*, 9901.

(182) Henkelman, G.; Jónsson, H. *J. Chem. Phys.* **2000**, *113*, 9978.

(183) Peters, B.; Heyden, A.; Bell, A. T.; Chakraborty, A. *J. Chem. Phys.* **2004**, *120*, 7877.

(184) Goodrow, A.; Bell, A. T.; Head-Gordon, M. *J. Chem. Phys.* **2009**, *130*, 244108.

(185) Goodrow, A.; Bell, A. T.; Head-Gordon, M. *Chem. Phys. Lett.* **2010**, *484*, 392–398.

(186) Zimmerman, P. *J. Chem. Theory Comput.* **2013**, *9*, 3043–3050.